

On Multivariate Singular Spectrum Analysis

ANISH AGARWAL ^{*}, Massachusetts Institute of Technology, USA

ABDULLAH ALOMAR^{*}, Massachusetts Institute of Technology, USA

DEVAVRAT SHAH^{*}, Massachusetts Institute of Technology, USA

We analyze a variant of multivariate singular spectrum analysis (mSSA), a widely used time series method used to impute (i.e., de-noise) and forecast a multivariate time series. Its restriction to a single time series, known as singular spectrum analysis (SSA), has been analyzed recently [1, 9]. Despite its popularity, theoretical understanding of mSSA is absent. Towards this we introduce a spatio-temporal factor model, a natural generalization of that considered in [9], to analyze mSSA. We establish the in-sample prediction error for both imputation and forecasting under mSSA scales as $1/\sqrt{NT}$, for N time series with T observations per time series. In contrast, for SSA the error scales as $1/\sqrt{T}$ and for popular matrix factorization based time series methods (c.f. [16, 26]), the error scales as $1/\min(N, T)$ – we note these previous results are established only for imputation. Thus mSSA naturally exploits both the ‘temporal’ and ‘spatial’ structure in a multivariate time series. We utilize an online learning framework to analyze the one-step-ahead prediction error of mSSA and establish it has a regret of $1/(\sqrt{NT}^{0.04})$ with respect to in-sample forecasting error. Empirically, we find mSSA outperforms neural network based time series methods, LSTM and DeepAR, two of the most widely used and empirically effective prediction methods used in practice, though they come with no theoretical guarantees of when and why they work. To establish our results, we make three technical contributions. First, we show that the “stacked” Page Matrix time series representation, the core data structure in mSSA, has an approximate low-rank structure for a large class of time series models used in practice under the spatio-temporal factor model we propose – in doing so, we introduce a ‘calculus’ for approximate low-rank models that mSSA works well for. In particular, we establish that such models are closed under linear combinations as well as multiplications. Second, to establish our regret bounds, we extend the theory of online convex optimization to when the constraints are time-varying, a variant not addressed by the current literature. Third, we extend the prediction error analysis of Principle Component Regression beyond the recent work of [2] to when the covariate matrix is approximately low-rank.

ACM Reference Format:

Anish Agarwal, Abdullah Alomar, and Devavrat Shah. 2020. On Multivariate Singular Spectrum Analysis. *J. ACM* 37, 4, Article 111 (August 2020), 41 pages. <https://doi.org/10.1145/1122445.1122456>

^{*}All authors are with Massachusetts Institute of Technology during the course of this work. Their affiliations include Department of EECS, LIDS, IDSS, Statistics and Data Science Center, and CSAIL.

Authors’ addresses: Anish Agarwal, anish90@mit.edu, Massachusetts Institute of Technology, MA, USA; Abdullah Alomar, aalomar@mit.edu, Massachusetts Institute of Technology, MA, USA; Devavrat Shah, devavrat@mit.edu, Massachusetts Institute of Technology, MA, USA.

Permission to make digital or hard copies of all or part of this work for personal or classroom use is granted without fee provided that copies are not made or distributed for profit or commercial advantage and that copies bear this notice and the full citation on the first page. Copyrights for components of this work owned by others than ACM must be honored. Abstracting with credit is permitted. To copy otherwise, or republish, to post on servers or to redistribute to lists, requires prior specific permission and/or a fee. Request permissions from permissions@acm.org.

© 2020 Association for Computing Machinery.

0004-5411/2020/8-ART111 \$15.00

<https://doi.org/10.1145/1122445.1122456>

CONTENTS

Abstract	1
Contents	2
1 Introduction	3
1.1 Multivariate Singular Spectrum Analysis	3
1.2 Our Contributions	4
1.3 Literature Review	6
1.4 Organization of Paper	7
2 Spatio-Temporal Factor Model For Multivariate Time Series	7
2.1 Spatio-Temporal Factor Model	7
2.2 Examples Of (G, ϵ) -Hankel Representable Time Series Dynamics	8
2.3 Stacked Hankel Matrix of mSSA is (Approximately) Low-Rank	10
3 mSSA Algorithm	11
3.1 mSSA Imputation and Forecasting: Mean Estimation	11
3.2 mSSA: An Online Convex Optimization Lens	12
4 Theoretical Results	14
4.1 Error Metrics for Evaluating Imputation and Forecasting Prediction Error	14
4.2 mSSA Mean Estimation - Finite Sample Analysis	15
4.3 mSSA Forecasting (Online Variant) - Regret Analysis	16
5 Experiments	17
5.1 Mean Estimation	17
5.2 Algorithms Parameters and Settings	19
6 Conclusion	20
References	21
A Proofs - (G, ϵ) -Hankel Representability of Different Time Series Dynamics	22
A.1 Proof of Proposition 2.1	22
A.2 Proof of Proposition 2.2	22
A.3 Proof of Proposition 2.4	22
A.4 Proof of Proposition 2.5	24
B Proofs - Stacked Hankel Matrix is Approximately Low-Rank	26
B.1 Helper Lemmas	26
B.2 Proof of Proposition 2.6	26
C Imputation and Forecasting Error Analysis - Proof Notation	27
C.1 Induced Linear Operator	27
D Concentration Inequalities Lemmas	28
E HSVT Error	30
F Proofs - Imputation Analysis	35
F.1 Proof of Theorem 4.1	35
G Proofs - Forecasting Analysis	35
G.1 Forecasting - Helper Lemmas	35
G.2 Proof of Theorem 4.2	38
H Proofs - Regret Analysis	38
H.1 Regret - Helper Lemmas	38
H.2 Proof of Theorem 4.3	41

1 INTRODUCTION

Multivariate time series data is of great interest across many application areas, including cyber-physical systems, finance, retail, healthcare to name a few. The goal across these domains can be summarized as accurate imputation and forecasting of a multivariate time series in the presence of noisy and/or missing data along with providing meaningful uncertainty estimates.

Setup. We consider a discrete time setting with time indexed as $t \in \mathbb{Z}$. Let $f_n : \mathbb{Z} \rightarrow \mathbb{R}$, $n \in [N] := \{1, \dots, N\}$ be the $N \in \mathbb{N}$ latent time series of interest. For $t \in [T]$ and $n \in [N]$, with probability $\rho \in (0, 1]$, we observe the random variable $X_n(t)$, where $X_n(t) = f_n(t) + \eta_n(t)$. While the underlying time series f_n is of course strongly correlated, we assume the per-step noise $\eta_n(t)$, are independent mean-zero random variables. We consider a time series model where $f_n(t)$ satisfies a spatio-temporal factor model as described in detail in Section 2.

Goal. The objective is two-folds: for $n \in [N]$, (i) imputation – estimating $f_n(t)$, for all $t \in [T]$; (ii) forecasting – learning a model to forecast $f_n(t)$ for $t > T$.

1.1 Multivariate Singular Spectrum Analysis

Singular Spectrum Analysis (SSA). We begin by describing SSA, a popular method in the literature for both imputation and forecasting (see [1, 9]) of a *univariate* time series. For the purposes of describing SSA, we assume access to only one time series $X_1(t)$. The variant of SSA considered in [1] performs three key steps: (a) transform $X_1(t)$, $t \in [T]$ into an $L \times T/L$ dimensional Page matrix by placing non-overlapping contiguous segments of size $L > 1$ (an algorithmic hyper-parameter) as columns¹; (b) perform Principal Component Analysis (PCA), or equivalently Hard Singular Value Thresholding (HSVT), on the resulting Page matrix (the number of principal components retained is an algorithmic hyper-parameter) to impute the time series; and (c) perform Ordinary Least Squares (OLS) on the retained principal components and the last row of the Page matrix to learn a linear forecasting model.

Multivariate Singular Spectrum Analysis (mSSA). Often, multiple related time series are available, e.g. prices of different stocks or sensor readings from cyber-physical systems. In this setting, the challenge is that one wants a method that both exploits the ‘temporal’ structure (i.e., the structure that exists *within* a time series) along with the ‘spatial’ structure (i.e., the structure that exists *across* the time series). Towards this goal, mSSA is a natural extension of the SSA method where in Step 1 of the algorithm, a “stacked” Page matrix of dimension $L \times (NT/L)$ is constructed from the multivariate time series data by concatenating (column-wise) the various Page matrices induced by each time series. The subsequent two steps of mSSA remain equivalent to the SSA method introduced above².

Why Study mSSA? First, mSSA is a very well established and heavily used in practice algorithm, yet lacks theoretical understanding. Second, we show that the variant of mSSA we propose has rather impressive empirical effectiveness. As seen in Table 2, despite mSSA’s simplicity, for both imputation and forecasting, it outperforms the current best deep learning based time series libraries on various time series benchmark datasets (see Section 5 for details on the experimental setup and the datasets used). Third, mSSA significantly outperforms SSA – thus somehow this

¹Formally, for a time series $f(t)$ with T observations, the Page Matrix induced by it $M^f \in \mathbb{R}^{L \times (T/L)}$ is defined as $M_{ij}^f := f(i + (j - 1)L)$; the Hankel Matrix induced by it $H^f \in \mathbb{R}^{L \times T}$ is defined as $H_{ij}^f := f(i + j - 1)$.

²The mSSA algorithm described is a variant of the standard SSA/mSSA method, (cf. [9]). However, the two core subroutines of performing PCA and subsequently OLS on the matrix induced from the time series remain the same. For a detailed comparison, please refer to our literature review.

Table 1. Comparison of finite-sample results with relevant algorithms in the literature.

Method	Functionality	Mean Estimation		Regret
		Multivariate time series	Imputation Forecasting	
This Work	Yes	$(NT)^{-\frac{1}{2}}$	$(NT)^{-\frac{1}{2}}$	$N^{-\frac{1}{2}}T^{-0.04}$
mSSA - Literature	Yes	—	—	—
SSA [1, 9]	No	$T^{-1/4}$	—	—
Neural Network [5, 17]	Yes	—	—	—
TRMF [16, 26]	Yes	$(\min(N, T))^{-1}$	—	—

seemingly arbitrary additional step of concatenating the various Page matrices together allows mSSA to exploit the additional “spatial” structure in the data that SSA cannot. This begs the question:

When and why does mSSA work?

1.2 Our Contributions

Theoretical Analysis of mSSA. In Section 4, we establish both the imputation and (in-sample) forecasting prediction error scale as $(NT)^{-1/2}$ (see Theorems 4.1 and 4.2). In particular, by first doing the core data transformation in mSSA of constructing the “stacked” Page matrix, we see the error scales as *the product of N and T*. Our analysis allows one to reason about the sample complexity gains by exploiting both the low-rank spatial structure amongst the multivariate time series and the temporal structure within each time series. For example, in [1] they establish that SSA has imputation error scaling as $T^{-\frac{1}{4}}$; in this paper, we do a tighter analysis of mSSA – of which SSA is a special case – that implies that SSA actually has imputation error scaling as $T^{-\frac{1}{2}}$. Still mSSA’s additional scaling given by the number of time series, N might explain why it has vastly superior empirical performance compared to SSA, as seen in Table 2. Further, recent results from the low-rank matrix factorization time series literature (see [16, 26]) show imputation error scales as $1/\min(N, T)$ (see Theorem 2 of [16]³); thus these methods do not show consistency with respect to imputation error unless *both* N and T are growing, e.g., they do not prove consistency if we only have access to a single ($N = 1$) time series. We also highlight that these previous works on SSA and matrix factorization do not prove consistency for forecasting error. See Table 1 for a summary of our theoretical results.

The time series prediction methods that are currently the most empirically effective in practice tend to be neural network (NN) based methods; in particular, LSTM (available through Keras – a standard deep learning library) and DeepAR [17] are some of the most popular. However, theoretical justification for when and why these NN-based approaches work for time series data is absent. That is why we restrict our comparisons to these methods to comprehensive empirical experiments (see Section 5). Pleasingly, mSSA outperforms these more complicated NN-based methods on standard time series benchmarks (see Table 2). Thus mSSA achieves best of both worlds, it comes with rigorous theoretical guarantees and has state-of-the-art empirical performance.

Approximate Low-Rank Hankel with Spatio-Temporal Factor Model. In Section 2.1, we propose a spatio-temporal factor model which provides a unifying view of two heavily-studied models from well-established yet disparate literatures - the factor model used for panel data (i.e., multivariate time series data) in econometrics, and the low-rank Hankel model in the SSA literature.

³There seems to be a typo in Corollary 2 of [26] in applying Theorem 2: square in Frobenius-norm error is missing.

Table 2. mSSA statistically outperforms SSA, other state-of-the-art algorithms, including LSTMs and DeepAR across many datasets. We use the average normalized root mean squared error (NRMSE) as our metric.

	Mean Imputation (NRMSE)				Mean Forecasting (NRMSE)			
	Electricity	Traffic	Synthetic	Financial	Electricity	Traffic	Synthetic	Financial
mSSA	0.391	0.494	0.253	0.283	0.483	0.525	0.196	0.358
SSA	0.519	0.608	0.626	0.466	0.552	0.704	0.522	0.592
LSTM	NA	NA	NA	NA	0.551	0.473	0.444	1.203
DeepAR	NA	NA	NA	NA	0.484	0.474	0.331	0.395
TRMF	0.694	0.512	0.325	0.513	0.534	0.570	0.267	0.464
Prophet	NA	NA	NA	NA	0.582	0.617	1.005	1.296

Under this model, in Proposition 2.6, we show the stacked Page (and Hankel) matrix, the key data representation in mSSA, is (approximately) low-rank. This is indeed the core reason why the, a priori, seemingly arbitrary stacked Page matrix transformation is well-motivated in mSSA.

Though restricting attention to time series that admit an approximate low-rank Hankel representation may a priori seem restrictive, as a contribution we establish in Section 2.2 that many important time series models have this approximate low-rank structure – e.g., any periodic differentiable function (a standard model in signal processing), any function with a holder continuous latent variable model representation (a standard model in statistics). Further, we develop a representation “calculus” of this model class by establishing that it is closed under component wise addition and multiplication (cf. Proposition 2.1). In doing so, we provide a more unified view of the representations established in [1]. Empirically, we find on real time series datasets that the stacked Page matrix does indeed have low-rank structure (see Table 3), and hence fits within our proposed model. We note that the spatio-temporal factor model we introduce is in line with that used in [26]. However, as stated above, it is the additional stacked Page matrix data transformation in mSSA which allows us prove the prediction error scales as the product of N and T rather than $\min(N, T)$ as in [26].

Online Variant of mSSA. Traditionally in time series analysis, the metric of evaluation is either parameter estimation, where explicit parametric assumptions are about the generating process, or the in-sample prediction error, which we provide bounds for. Analyzing how well time series methods “generalize”, i.e., what is the quality of one-step ahead forecasts, remains a challenging task. Traditional techniques to analyze generalization such as Rademacher analysis ([3]) requires that underlying data generating process produces independent and identically distributed (i.i.d) samples, which clearly does not hold in our setting – see Section 3.2 for a detailed discussion on this point. Towards understanding the quality of mSSA’s one-step ahead forecasts, we propose an online variant of mSSA and establish it has regret scaling as $N^{-\frac{1}{2}}T^{-0.04}$ (see Corollary 4.1). To do so, we establish an online variant of Principle Component Regression, a key step in the mSSA algorithm, has sub-linear regret in an error-in-variable regression setting. Technically, this required extending the theory of online convex optimization (OCO) to deal with time-varying constraints, i.e., the decision set is changing per time step. This is a variation *not addressed* by existing analysis on OCO – see for example [13] which provides an overview of state-of-art results for OCO. This additional complication of having time-varying constraints is why we have a suboptimal rate of regret with respect to the scaling in T . Seeing whether we can match the optimal rate of $(NT)^{-1/2}$, achieved in traditional OCO, for the more involved setting we consider remains as important direction for future research. Also, connecting our setting to the recent exciting line of work on Sequential Rademacher analysis ([15]) remains an interesting future direction of work.

1.3 Literature Review

Given the ubiquity of multivariate time series analysis, we cannot possibly do justice to the entire literature. Hence we focus on a few techniques, most relevant to compare against, either theoretically or empirically.

SSA. For a detailed analysis of the standard SSA method, please refer to [9]. The main steps of SSA are given by: Step 1 - create a Hankel matrix from the time series data; Step 2 - do a Singular Value Decomposition (SVD) of it; Step 3 - group the singular values based on user belief of the model that generated the process; Step 4 - perform diagonal averaging to “Hankelize” the grouped rank-1 matrices outputted from the SVD to create a set of time series; Step 5 - learn a linear model for each “Hankelized” time series for the purpose of forecasting. The theoretical analysis of this original SSA method has been on proving that many univariate time series have a low-rank Hankel representation, and secondly on defining sufficient *asymptotic* conditions for when the singular values of the various time series components are separable, thereby justifying Step 3 of the method.

In [1], the authors extend the class of time series considered to those with an approximate low-rank Hankel structure. Some subtle but core alterations to the SSA procedure were made. In Step 1, the Page Matrix rather than the Hankel was used, which allowed for independent noise assumptions to hold. In Steps 2-3, instead of doing the SVD of the matrix and grouping the singular values, only a single threshold is picked for the singular values (i.e., simply doing H SVD on the induced Page matrix). In Step 4, subsequently, a single linear forecasting model is learnt rather than a separate linear forecaster for each grouped time series. Under such a setting, they perform a finite-sample analysis of the variant of SSA. However the analysis in [1] does falls short, even for the univariate case, as they *do not explicitly show consistency of the SSA estimator for forecasting*.

mSSA. mSSA is the natural extension of SSA for multivariate time series data and has been employed in a variety of applications with some empirical success (see [11, 12, 14]). However, theoretical analysis or even practical guidance regarding when and why it works is severely limited.

Matrix Based Multivariate Time Series Methods. There is a recent line of work in time series analysis (see [23, 26]), where multiple time series are viewed collectively as a matrix and some form of matrix factorization is done. Most such methods make strong prior model assumptions on the underlying time series and the algorithm changes based on assumptions of the time series dynamics that generated the data. Further finite sample analysis, especially with respect to forecasting error, of such methods is usually lacking. We highlight one method, Temporal Regularized Matrix Factorization (TRMF) (see [26]), which we directly compare against due to its popularity, and as it achieves state-of-the-art imputation and forecasting empirical performance. In [26], authors provide finite sample imputation analysis for an instance of the model considered in this work. In addition to the model being restrictive, the imputation error scales as $1/\min(N, T)$ which is weaker compared to our imputation error of $1/\sqrt{NT}$. For example, for $N = \Theta(1)$, their error bound remains $\Theta(1)$ for any T , while that of mSSA would vanish as T grows.

Other Relevant Time Series Methods. With the advent of deep learning, neural network (NN) based approaches have been the most popular and empirically effective. Some industry standard neural network methods include LSTMs, from the Keras library (a standard NN library, see [5]) and DeepAR (an industry leading NN library for time series analysis, see [17]).

Panel Data Models – Econometrics. In a traditional panel data factor model in econometrics, for $n \in [N]$ and $t \in \mathbb{Z}$, $X_n(t) = \sum_{r=1}^R U_{nr} W_{tr} + \eta_{tn}$, where $U_{n, \cdot}, W_{t, \cdot} \in \mathbb{R}^R$ for some fixed $R \geq 1$. The R -dimensional vectors $U_{n, \cdot}, W_{t, \cdot}$ are referred to as the low-dimensional “factor loadings” associated with time and “space” respectively, and $\eta_{n,t}$ is independent noise per measurement. Despite the

ubiquity of such factor models for multivariate time series data, the time series dynamics associated with the latent factors W_{tr} are not explicitly modeled. In the model we propose, we exploit this additional structure by considering a time series model class for each latent time series factor, $W_{r,r} \in \mathbb{R}^T$ for $r \in [R]$. In particular, we consider a time series model class where the Hankel matrix induced by each $W_{r,r}$ has an approximate low-rank structure (see Definition 2.1). This (approximate) low-rank Hankel model class is inspired and extended from the SSA literature (see [1, 9]). We show that this approximate low-rank Hankel representation includes many important time series dynamics such as: any finite sum and products of harmonics and polynomials; any differentiable periodic function; any time series with a sufficiently “smooth” non-linear latent variable model representation (see Section 2.2). In short, this spatio-temporal factor model we propose can be thought of as a synthesis of two standard time series models: (1) a low-rank factor model traditionally used to analyze multivariate time series data in the econometrics literature; (2) approximately low-rank Hankel models for “time factors”, a representation traditionally used to analyze univariate time series data in the SSA literature. Details of the model we propose can be found in Section 2.

1.4 Organization of Paper

In Section 2, we introduce a spatio-temporal model for multivariate time series under which mSSA is effective. In Section 3, we detail the mSSA algorithm, in particular how to use it to do imputation and forecasting; we also introduce an online variant of mSSA which produces one-step-ahead forecasts in an online fashion. In Section 4, we provide our finite-sample-analysis of mSSA with respect to imputation and forecasting; we also establish regret bounds for the online variant of mSSA we introduce. Lastly in Section 5, we detail the empirical experiments we run to produce the results in Table 2.

2 SPATIO-TEMPORAL FACTOR MODEL FOR MULTIVARIATE TIME SERIES

This section is organized into three parts: (i) Section 2.1 describes the spatio-temporal factor model we introduce; (ii) Section 2.2 describes the family of time series dynamics we consider for the latent factors associated with time; (iii) Section 2.3 shows theoretically and empirically that the stacked Page (and Hankel) matrix induced as a result of the core data transformation of mSSA is (approximately) low-rank.

2.1 Spatio-Temporal Factor Model

Spatio-Temporal Factor Model for Latent Multivariate Time-Varying Mean. Define $\mathcal{M}^f \in \mathbb{R}^{N \times T}$ as $\mathcal{M}_n^f(t) = f_n(t)$. We posit the following spatio-temporal factor model,

PROPERTY 2.1. *Let \mathcal{M}^f satisfy $\mathcal{M}_n^f(t) = \sum_{r=1}^R U_{nr}^f W_r^f(t)$, where $W_r^f(\cdot) : \mathbb{Z} \rightarrow \mathbb{R}$, $|U_{nr}^f| \leq \Gamma_1$, $|W_r^f(\cdot)| \leq \Gamma_2$.*

Interpretation. There are R “fundamental” time series denoted by $W_r^f(\cdot) : \mathbb{Z} \rightarrow \mathbb{R}$, $r \in [R]$. For each $n \in [N]$, $\mathcal{M}_n^f(\cdot)$ is obtained through a weighted combination of these R times series, where the weights are given by U_{nr}^f . Γ_1, Γ_2 are standard boundedness assumptions for the underlying latent time-varying means. As noted in Section 1.3, in the econometrics literature particularly to model panel data, the R -dimensional vectors $U_{n,\cdot}, W_{t,\cdot}$ are referred to as the low-dimensional “factor loadings” associated with “space” and time respectively; $\eta_{n,t}$ is the independent noise per measurement. Despite the ubiquity of such factor models in time series analysis, the time series dynamics associated with the latent factors W_{tr} are not explicitly modeled. This is exactly what a

spatio-temporal model aims to circumvent. We specify and motivate the class of time series models we consider for $W_r^f(\cdot)$ below.

Time Series Model Class Considered: (G, ϵ) -Hankel Representable Time Series. Below, we describe the approximately low-rank Hankel model we consider for the latent time series factors, $W_r^f(\cdot)$.

DEFINITION 2.1. For any $T \geq 1$, let the Hankel matrix $\mathbf{H}^f \in \mathbb{R}^{T \times T}$ induced by a time series f be defined as $H_{ij}^f := f(i + j - 1)$, $i, j \in [T]$. A time series f is said to be (G, ϵ) -Hankel representable if there exists $\mathbf{H}_{(lr)}^f \in \mathbb{R}^{T \times T}$, such that (i) $\text{rank}(\mathbf{H}_{(lr)}^f) \leq G$; (ii) $\|\mathbf{H}^f - \mathbf{H}_{(lr)}^f\|_{\max} \leq \epsilon$.

PROPERTY 2.2. For $r \in [R]$, $W_r^f(\cdot)$ is (G_r^f, ϵ_r^f) -Hankel, where $G_r^f \leq G_{\max}$, $|\epsilon_r^f| \leq \epsilon_{\max}$.

Section 2.2 establishes that a large class of models admit such a (G, ϵ) -Hankel representation.

Noisy, Sparse Observation Model. We now state some assumptions on how the observations of \mathcal{M}^f are corrupted by noise and missingness.

PROPERTY 2.3. For $(n, t) \in [N] \times [T]$ and $\rho \in (0, 1]$, we observe $\tilde{X}_n(t)$ where $\tilde{X}_n(t) = X_n(t)$ with probability ρ and \star with probability $1 - \rho$.

PROPERTY 2.4. $\eta_n(t)$ are independent mean-zero sub-gaussian random variables, where $\|\eta_n(t)\|_{\psi_2} \leq \gamma$.

2.2 Examples Of (G, ϵ) -Hankel Representable Time Series Dynamics

In this section, we show this approximate low-rank Hankel representation includes many important time series dynamics considered in the literature, including: (i) any finite sum of harmonics, polynomials and exponentials (Proposition 2.3); (ii) any differentiable periodic function (Proposition 2.4) – we note, this is a heavily utilized time series model in signal processing; (iii) any time series with a Holder continuous non-linear latent variable model Hankel representation (Proposition 2.5). Furthermore, we show the class of (G, ϵ) -Hankel representable time series is closed under component wise addition and multiplication (Proposition 2.1). *Importantly, we establish the more measurements we collect (i.e., as T grows), the approximation error for all these time series dynamics decays to zero.*

2.2.1 (G, ϵ) -Hankel Time Series “Calculus”.

Sums of Time Series. For two time series f_1 and f_2 , let $f_1 + f_2$ represent the time series induced by adding the values of the time series f_1 and f_2 component wise, i.e., $(f_1 + f_2)(t) = f_1(t) + f_2(t)$ for all $t \in \mathbb{Z}$.

Products of Time Series. For two time series f_1 and f_2 , let $f_1 \circ f_2$ represent the time series induced by multiplying the values of the time series f_1 and f_2 component wise, i.e., $(f_1 \circ f_2)(t) = f_1(t) \times f_2(t)$ for all $t \in \mathbb{Z}$.

In the following proposition we establish that time series representable as (G, ϵ) -Hankel time series are “closed” under component wise sums and products.

PROPOSITION 2.1. Let f_1 and f_2 be two time series which are (G_1, ϵ_1) -Hankel and (G_2, ϵ_2) -Hankel representable respectively. Then $f_1 + f_2$ is a $(G_1 + G_2, \epsilon_1 + \epsilon_2)$ -Hankel. And, $f_1 \circ f_2$ is a $(G_1 G_2, 3 \max(\epsilon_1, \epsilon_2) \cdot \max(\|f_1\|_{\infty}, \|f_2\|_{\infty}))$ -Hankel.

See Appendix A.1 for proof of Proposition 2.1.

2.2.2 (G, ϵ) -LRF Time Series.

DEFINITION 2.2 $((G, \epsilon)\text{-LRF})$. For $G \in \mathbb{N}$ and $\epsilon > 0$, a time series f is said to be a (G, ϵ) -Linear Recurrent Formula (LRF) if for all $T \in \mathbb{Z}$ and $t \in [T]$, there exists $g : \mathbb{Z} \rightarrow \mathbb{R}$ such that

$$f(t) = g(t) + \epsilon(t),$$

where for all $t \in \mathbb{Z}$: (i) $g(t) = \sum_{l=1}^G \alpha_l g(t-l)$ with constants $\alpha_1, \dots, \alpha_G$; (ii) $|\epsilon(t)| \leq \epsilon$.

Now we establish (G, ϵ) -LRFs are (G, ϵ) -Hankel representable (see Appendix A.2 for proof).

PROPOSITION 2.2. If f is a time series is (G, ϵ) -LRF representable, then it is (G, ϵ) -Hankel representable.

Finite Product of Harmonics, Polynomials and Exponentials. LRF's cover a broad class of time series functions, including any finite sum of products of harmonics, polynomials and exponentials. The order G of the LRF induced by such a time series is quantified through the following proposition.

PROPOSITION 2.3. (Proposition 5.2 in [1]) Let P_{m_a} denote a polynomial of degree m_a . Then,

$$f(t) = \sum_{a=1}^A \exp(\alpha_a t) \cdot \cos(2\pi\omega_a t + \phi_a) \cdot P_{m_a}(t)$$

is $(G, 0)$ -LRF representable, where $G \leq A(m_{\max} + 1)(m_{\max} + 2)$, where $m_{\max} = \max_{a \in A} m_a$.

REMARK 2.1. Given a time series of K harmonics, the order of the LRF induced by it is independent of the period of the K harmonics. Rather, the order of the LRF scales only with the number of harmonics.

2.2.3 “Smooth”, Periodic Time Series - $C_{T\text{-per}}^k$.

Here we establish, perhaps surprisingly, that any differentiable periodic function – specifically a time series in $C_{T\text{-per}}^k$ as in Definition 2.3 below – has a (G, ϵ) -LRF representation. Intuitively, this is possible as by Fourier analysis it is well-established that such functions are well-approximated by finite sums of harmonics, which themselves are LRFs as stated in Proposition 2.3.

DEFINITION 2.3 ($C_{R\text{-per}}^k$ -SMOOTHNESS). A time series f is said to be in $C_{R\text{-per}}^k$ -smooth if f is R' -periodic (i.e. $f(t + R') = f(t)$) and the k -th derivative of f , denoted $f^{(k)}$, exists and is continuous.

PROPOSITION 2.4. Let f be a time series such that $f \in C_{R\text{-per}}^k$. Then for any $G \in \mathbb{N}$, f is

$$\left(4G, C(k, R') \frac{\|f^{(k)}\|}{G^{k-0.5}}\right) - \text{Hankel representable.}$$

Here $C(k, R')$ is a term that depends only on k, R' ; and $\|f^{(k)}\|^2 = \frac{1}{R'} \int_0^{R'} (f^{(k)}(t))^2 dt$.

See Appendix A.3 for proof of Proposition 2.4.

2.2.4 Time Series with Latent Variable Model Structure.

Time Series with Latent Variable Model (LVM) Representations. We now show that if a time series has a Latent Variable Model (LVM) representation, and the latent function is Hölder continuous, then it has a (G, ϵ) -Hankel representation. We first define the Hölder class of functions. Note this class of functions is widely adopted in the non-parametric regression literature [21]. Given a function $g : [0, 1]^K \rightarrow \mathbb{R}$, and a multi-index $\kappa \in \mathbb{N}^K$, let the partial derivative of g at $x \in [0, 1]^K$, if it exists, be denoted as $\nabla_\kappa g(x) = \frac{\partial^{|\kappa|} g(x)}{(\partial x)^\kappa}$ where $|\kappa| = \sum_{j=1}^K \kappa_j$ and $(\partial x)^\kappa = \partial^{\kappa_1} x_1 \cdots \partial^{\kappa_K} x_K$.

DEFINITION 2.4 ((α, \mathcal{L})-HÖLDER CLASS). Let α, \mathcal{L} be two positive numbers. The Hölder class $\mathcal{H}(\alpha, \mathcal{L})$ on $[0, 1]^K$ ⁴ is defined as the set of functions $g : [0, 1]^K \rightarrow \mathbb{R}$ whose partial derivatives satisfy for all $x, x' \in [0, 1]^K$,

$$\sum_{\kappa: |\kappa|=\lfloor \alpha \rfloor} \frac{1}{\kappa!} |\nabla_\kappa g(x) - \nabla_\kappa g(x')| \leq \mathcal{L} \|x - x'\|_\infty^{\alpha - \lfloor \alpha \rfloor}. \quad (1)$$

Here $\lfloor \alpha \rfloor$ refers to the greatest integer strictly smaller than α and $\kappa! = \prod_{j=1}^K \kappa_j!$.

REMARK 2.2. Note if $\alpha \in (0, 1]$, then (1) is equivalent to the (α, \mathcal{L}) -Lipschitz condition, i.e. for all $x, x' \in [0, 1]^K$

$$|g(x) - g(x')| \leq \mathcal{L} \|x - x'\|_\infty^\alpha.$$

PROPERTY 2.5 (TIME SERIES WITH (α, \mathcal{L}) -HÖLDER SMOOTH LVM REPRESENTATION). Let $H^f \in \mathbb{R}^{T \times T}$ be the Hankel matrix induced by a time series f . Recall $H_{t,s}^f := f(t+s-1)$. A time series f is said to have a (α, \mathcal{L}) -Hölder Smooth LVM Representation if for each $T \in \mathbb{N}$, the Hankel matrix, H^f , has the following representation

$$H_{t,s}^f = g(\theta_t, \omega_s),$$

where $\theta_t, \omega_s \in [0, 1]^K$ are latent parameters. Moreover for all $\omega_s, g(\cdot, \omega_s) \in \mathcal{H}(\alpha, \mathcal{L})$ as defined in (1).

As stated earlier, the domain of the latent parameters θ_t, ω_s in Property 2.5 is easily extended to any compact subset of \mathbb{R}^K by appropriate rescaling.

REMARK 2.3. Note that a $(G, 0)$ -Hankel denoted by f has the following representation (see Proposition B.2),

$$H_{ij}^f = (a^{(i)})^T b^{(j)},$$

for some latent vectors $a^{(i)}, b^{(j)} \in \mathbb{R}^G$. Hence, a $(G, 0)$ -Hankel representable time series is an instance of a time series that satisfies Property 2.5 for all $\alpha \in \mathbb{N}$, and $\mathcal{L} = C$, for some absolute positive constant, C . One can thus think of time series that satisfy Property 2.5 as generalizations to sufficiently smooth non-linear functions, instead of just bilinear products of the latent factors.

PROPOSITION 2.5. Let a time series f satisfy Property 2.5 with parameters α, \mathcal{L} . Then for all $\epsilon > 0$, f is

$$(C(\alpha, K) \left(\frac{1}{\epsilon} \right)^K, \mathcal{L} \epsilon^\alpha) - \text{Hankel representable}.$$

Here $C(\alpha, K)$ is a term that depends only on α and K .

See Appendix A.4 for proof of Proposition 2.5.

2.3 Stacked Hankel Matrix of mSSA is (Approximately) Low-Rank

Stacked Page, Hankel Matrix Notation. The notation below is a formal description of the stacked Page and Hankel matrices one gets by performing the core mSSA data transformation, i.e., concatenating the induced matrices column-wise. The only difference is the stacked Hankel matrix contains overlapping columns while the stacked Page matrix (utilized in the proposed variant of mSSA) does not. For a multivariate time series f with N time series and T observations, let $L \in \mathbb{N}$ be a hyper-parameter and let $P = \lfloor T/L \rfloor$. For simplicity, throughout we shall assume that $T/L = \lfloor T/L \rfloor$, i.e., $L \times P = T$. Let $\bar{P} := N \times P$. Let $M^f \in \mathbb{R}^{L \times \bar{P}}$, $H^f \in \mathbb{R}^{L \times (N \times (T-L+1))}$ be the induced stacked Page

⁴The domain is easily extended to any compact subset of \mathbb{R}^K .

and Hankel matrices by f (with hyper-parameter $L \geq 1$); for $l \in [L]$, $k_1 \in [P]$, $k_2 \in [T - L + 1]$, $n \in [N]$,

$$\mathbf{M}_{l,[k_1+P \times (n-1)]}^f = f_n(l + (k_1 - 1)L), \quad \mathbf{H}_{l,[k_2+(T-L+1) \times (n-1)]}^f = f_n(l + k_2 - 1).$$

Theoretical Justification For Stacked Hankel Matrix Transformation. Proposition 2.6 shows that the stacked Page and Hankel matrices, the core data structures of interest in mSSA, have an approximate low-rank representation under our proposed model. This approximate low-rank structure of \mathbf{H}^f is what crucially allows us to connect the analysis mSSA to recent advances in matrix estimation and high-dimensional statistics. See Appendix B for a proof of Proposition 2.6.

PROPOSITION 2.6. *Let Properties 2.1 and 2.2 hold. Let $\mathbf{M}^f, \mathbf{H}^f$ be defined w.r.t \mathbf{M}^f . Then there exists a matrix $\mathbf{H}_{(lr)}^f$ such that, $\text{rank}(\mathbf{H}_{(lr)}^f) \leq RG_{\max}$, and $\|\mathbf{H}^f - \mathbf{H}_{(lr)}^f\|_{\max} \leq R\epsilon_{\max}\Gamma_1$. As an immediate consequence, there exists $\mathbf{M}_{(lr)}^f$ such that $\text{rank}(\mathbf{M}_{(lr)}^f) \leq RG_{\max}$ and $\|\mathbf{M}^f - \mathbf{M}_{(lr)}^f\|_{\max} \leq R\epsilon_{\max}\Gamma_1$.*

Interpretation. We see that the stacked Hankel matrix has (approximate) rank no larger than the product of the rank of the factor model, R , and the maximum (approximate) rank, G_{\max} , of the Hankel matrices induced by the latent factors $W_r^f(\cdot)$ for $r \in [R]$. Crucially, the rank does not scale with the number of time series, N , nor with the number of measurements, T . Indeed we see in Table 3 that across standard benchmark datasets, detailed in Section 5, the (approximate) rank of the stacked Hankel matrix indeed scales very slowly with the number of time series, N and number of measurements, T . Hence these standard multivariate time series datasets seem to fit within our proposed spatio-temporal model.

Table 3. Across standard benchmarks, effective rank of the stacked Hankel matrix (\mathbf{H}^X) scales slowly with the number of time series. Effective rank is defined as the number of singular values to capture $> 90\%$ of the spectral energy.

Dataset	N = 1	N = 10	N = 100	N = 350
Electricity	19	37	44	31
Financial	1	3	3	6
Traffic	14	32	69	116

3 MSSA ALGORITHM

Some Necessary Notation. Recall from Section 2.1, we observe $\tilde{X}_n(1 : T) \in \mathbb{R}^T$ for $n \in [N]$. Additionally, let $\hat{\rho}$ denote the fraction of observed entries, i.e., $\hat{\rho} := \frac{1}{NT} \left(\sum_{(n,t) \in [N] \times [T]} \mathbb{1}(\tilde{X}_n(t)) \neq \star \right) \vee \frac{1}{NT}$. For a matrix $\mathbf{A} \in \mathbb{R}^{L \times \bar{P}}$, let $\mathbf{A}_L \in \mathbb{R}^{\bar{P}}$ refer to the last row of \mathbf{A} and let $\bar{\mathbf{A}} \in \mathbb{R}^{(L-1) \times \bar{P}}$ refer to the sub-matrix induced by retaining its first $L - 1$ rows.

3.1 mSSA Imputation and Forecasting: Mean Estimation

Mean Estimation Algorithm. Parameters are $L \geq 1, k \geq 1$.

Imputation. The key steps of mean imputation are as follows.

1. (Form Page Matrix) Transform $\tilde{X}_1(1 : T), \dots, \tilde{X}_N(1 : T)$ into a stacked Page matrix $Z^X \in \mathbb{R}^{L \times \bar{P}}$ with $L \leq \bar{P}$. Fill all missing entries in the matrix by 0.

2. (Singular Value Thresholding) Let SVD of $Z^X = USV^T$, where $U \in \mathbb{R}^{L \times L}$, $V \in \mathbb{R}^{\bar{P} \times L}$ represent left, right singular vectors, $S = \text{diag}(s_1, \dots, s_L)$ is diagonal matrix of singular values $s_1 \geq \dots \geq s_L \geq 0$. Obtain $\hat{M}^{f(\text{Impute})} = US_k V^T$ where, $S_k = \text{diag}(s_1, \dots, s_k, 0, \dots, 0)$ for some $k \in [L]$.
3. (Output) $\hat{f}_n(i + (j-1)L) := \hat{M}_{i, [j+P(n-1)]}^{f(\text{Impute})}$, $i \in [L]$, $j \in [P]$, $n \in [N]$.

Forecasting. Forecasting includes an additional step of fitting a linear model on the de-noised matrix.

1. (Form Sub-Matrices) Let $\bar{Z}^X \in \mathbb{R}^{L-1 \times \bar{P}}$ be a sub-matrix of Z^X obtained by removing its last row, Z_L^X .
2. (Singular Value Thresholding) Let SVD of $\bar{Z}^X = \bar{U} \bar{S} \bar{V}^T$, where $\bar{U} \in \mathbb{R}^{L-1 \times L-1}$, $\bar{V} \in \mathbb{R}^{\bar{P} \times L-1}$ represent left and right singular vectors and $\bar{S} = \text{diag}(s_1, \dots, s_{L-1})$ be diagonal matrix of singular values $\bar{s}_1 \geq \dots \geq \bar{s}_{L-1} \geq 0$. Obtain $\hat{M}^f = \bar{U} \bar{S}_k \bar{V}^T$ by setting all but top k singular values to 0, i.e. $\bar{S}_k = \text{diag}(\bar{s}_1, \dots, \bar{s}_k, 0, \dots, 0)$ for some $k \in [L-1]$.
3. (Linear Regression) $\hat{\beta} \in \arg \min_{b \in \mathbb{R}^{L-1}} \|Z_L^X - (\hat{M}^f)^T b\|_2^2$.
4. (Output) For $s \in \{L, 2L, \dots\}$, $n \in [N]$, $\hat{f}_n(s) := X_n(s-L+1 : s-1)^T \hat{\beta}$ ⁵.

3.2 mSSA: An Online Convex Optimization Lens

In Theorem 4.2, we establish that the mSSA algorithm described in Section 3 has small in-sample forecasting error. In contrast, in this section we are interested in evaluating mSSA’s performance in one-step-ahead forecasting, i.e., ‘out-of-sample’ performance. In a traditional prediction or supervised learning framework, the out-of-sample performance or ‘generalization error’ of an algorithm is evaluated by assuming that the out-of-sample (or test) observations obeys similar distributional properties to the in-sample (or training) observations. In the context of time series analysis, such a setup is particularly ill suited as the distributional properties of time series data is constantly changing as we collect more data, precisely because it is time-varying. For example, in mSSA we view an observation at a particular time step as a ‘label’ and the observations at the time steps immediately preceding it as ‘features’ – a forecasting estimator is then learnt by fitting an appropriate linear function to these features and labels. However in our setting, this feature and label tuple is changing with time and thus we cannot assume each such tuple identically distributed. Thus we need an alternative framework to reason about out-of-sample performance in time series forecasting analysis. Towards this goal, to quantify mSSA’s out-of-sample performance, we utilize an online convex optimization (OCO) framework, albeit with an important difference from the OCO setup traditionally considered in the literature. We exposit on this next.

Online Convex Optimization (OCO) Setup. The aim of this section is to formally tie mSSA to an OCO setting. First, we briefly describe the setup/dynamics of OCO relevant to us. At each step, $t \in \mathbb{N}$ we receive a convex set Ω_t and choose an element in it, denoted as $\beta_t \in \Omega_t$. Subsequent to choosing β_t , we receive cost function c_t and incur cost $c_t(\beta_t)$. *Note the key difference from the tradition OCO setup is that the convex set Ω_t is varying over time, an area of limited study in the online learning literature (see [13]).*

Setup and Notation for online-mSSA. Recall the definition of $\tilde{X}_n(t)$ from Property 2.3. For the remainder of this section, we assume that there are no missing values, i.e., $\tilde{X}_n(t) = X_n(t)$ for $n \in [N]$ and $t \in [T]$. As before, let $t \in \mathbb{N}$ denote the time index and let $n \in [N]$ denote the index of each time series. We shall reveal the observations of each of the N time series for a given time t one-by-one, in a fixed but arbitrary order. That is, before we start observing time step t for any

⁵For Section 4, we denote $\hat{M}_L^{f(\text{Forecast})} \in \mathbb{R}^P$ as $\hat{M}_L^{f(\text{Forecast})}(s + (n-1)P) := \hat{f}_n(s)$ for $n \in [N]$, $s \in [P]$

of the N time series, we have observed *all* observations associated with all time series till time $t - 1$. Specifically, let $(t, n) \in \mathbb{N} \times [N]$ be a double index denoting observation of the n th time series at time t . Note at index (t, n) we have $(t - 1)N + n$ observations. Let the stacked Page matrix induced by the first (t, n) observations be denoted as $Z_{(t,n)}^X \in \mathbb{R}^{L \times \lfloor ((N(t-1)+n)/L) \rfloor}$ – as before, for simplicity and without loss of generality, we assume $\lfloor ((N(t-1)+n)/L) \rfloor = ((N(t-1)+n)/L)$ – where $[Z_{(t,n)}^X]_{i,j} = X_{(j-N\lfloor j/N \rfloor)}(i + L\lfloor j/N \rfloor)$ ⁶. Let $[Z_{(t,n)}^X]_L$ refer to the last row of the stacked Page matrix and let $\bar{Z}_{(t,n)}^X$ be the sub-matrix of $Z_{(t,n)}^X$ obtained by removing the last row, $[Z_{(t,n)}^X]_L$. For any $k \in [L - 1]$, let $\bar{U}_{(t,n)}^k \in \mathbb{R}^{(L-1) \times k}$ refer to the first k left singular vectors of $\bar{Z}_{(t,n)}^X$. Let $\Omega_{(t,n)}^k$ refer to the linear subspace induced by $\bar{U}_{(t,n)}^k$.

mSSA as Regularized Linear Regression. For $(t, n) \in \mathbb{N} \times [N]$, if we ran the forecasting algorithm in Section 3.1 with all available data, define $\beta_{(t,n)}^*$ as the resulting linear model obtained (i.e., $\hat{\beta}$ from Step 3 of the forecasting algorithm in Section 3.1). For any fixed $k \in [L - 1]$, where k is the number of singular vectors of $\bar{Z}_{(t,n)}^X$ retained, it can easily be verified that the $\beta_{(t,n)}^*$ is the solution of

$$\beta_{(t,n)}^* = \arg \min_{b \in \Omega_{(t,n)}^k} \|[Z_{(t,n)}^X]_L - (\bar{Z}_{(t,n)}^X)^T b\|_2^2. \quad (2)$$

Interpretation. The $\hat{\beta}$ produced in the forecasting algorithm in Section 3.1 is learnt by applying Principal Component Regression (PCR) on the stacked Page matrix, see Proposition 3.1 of [2] for example. It is a standard result that PCR is a form of regularized linear regression where the linear model $\beta_{(t,n)}^*$ is constrained to lie in the subspace spanned by the first k singular vectors (i.e., $\Omega_{(t,n)}^k$), of the covariate matrix (i.e., $\bar{Z}_{(t,n)}^X$).

OCO Dynamics for mSSA Setting. We make the following assumptions: (i) we have access to T data points for each of the N time series before we start making one-step ahead forecasts using mSSA; (ii) for each time series $n \in [N]$, we make a forecast for H time steps at points $\{T + L, T + 2L, \dots, T + H \times L\}$ ⁷; (iii) we assume k the number of principal components we retain at each step is also specified beforehand (hence, $\Omega_{(T+tL,n)}^k$ for $t \in [H]$ is the induced convex set from which we pick the per step linear model). We can now specify the OCO framework for our mSSA setting.

For $n \in [N]$ and for $t \in [H]$:

1. Pick $\hat{\beta}_{(T+tL,n)}$ from $\Omega_{(T+tL,n)}^k$;
2. Incur cost $c_{(T+tL,n)}(\hat{\beta}_{(T+tL,n)}) := [X_n(T + tL) - (X_n(T + (t - 1)L + 1 : T + tL - 1))^T \hat{\beta}_{(T+tL,n)}]^2$.

online-mSSA. We shall utilize an online gradient descent variant of the mSSA algorithm: for $n \in [N]$,

1. Initialize $\hat{\beta}_{(T+L,n)}$, compute cost $c_{(T+L,n)}(\hat{\beta}_{(T+L,n)})$.
2. Update, $t \in [1 : H]$ as:

$$\text{i)} \quad \tilde{\hat{\beta}}_{(T+(t+1)L,n)} = \hat{\beta}_{(T+tL,n)} - \delta \nabla c_{(T+tL,n)}(\hat{\beta}_{(T+tL,n)});$$

⁶In words, we stack the first L observations of the time series $X_1(\cdot), X_2(\cdot), \dots, X_N(\cdot)$ column-wise to construct the first N columns of $Z_{(t,n)}^X$. Then using the $L + 1$ to $2L$ observations of $X_1(\cdot), X_2(\cdot), \dots, X_N(\cdot)$, we construct the next N columns of $Z_{(t,n)}^X$, and so on.

⁷We make forecasts at multiples of L . This is easily circumvented by having L different models; for ease of exposition, we keep it to only single model.

$$\text{ii) } \hat{\beta}_{(T+(t+1)L,n)} = \operatorname{argmin}_{w \in \Omega_{(T+(t+1)L,n)}^k} \|w - \tilde{\hat{\beta}}_{(T+(t+1)L,n)}\|_2.$$

Algorithm Intuition. In effect, we utilize the standard projected online gradient descent algorithm. As stated earlier, the key difference is in our setting, the domain $\Omega_{(t,n)}^k$ is changing at each time step. We give guidance on choice of δ when instantiating the regret bound in Theorem 4.1.

4 THEORETICAL RESULTS

From Section 2.3, recall definition of $L, P, \bar{P}, M^f, M_L^f$ and \bar{M}^f .

4.1 Error Metrics for Evaluating Imputation and Forecasting Prediction Error

Imputation. For an estimate $\hat{M}^{f(\text{Impute})}$ of M^f , our imputation error metric is

$$\text{MSE}(M^f, \hat{M}^{f(\text{Impute})}) := \frac{1}{NT} \mathbb{E} \|M^f - \hat{M}^{f(\text{Impute})}\|_F^2,$$

where the expectation is over noise and $\|\cdot\|_F$ refers to the Frobenius norm.

Forecasting. For forecasting we evaluate mSSA through two error metrics, the in-sample prediction error and an online regret analysis.

In-Sample Prediction Error. Recall $M_L^f \in \mathbb{R}^{\bar{P}}$ refers to the last row of the induced stacked Page matrix. For an estimate $\hat{M}_L^{f(\text{Forecast})}$, we define the *in-sample* prediction error with respect to M_L^f as⁸

$$\text{MSE}(M^f, \hat{M}^{f(\text{Forecast})}) := \frac{1}{\bar{P}} \mathbb{E} \|M_L^f - \hat{M}_L^{f(\text{Forecast})}\|_2^2.$$

Regret Metric. Recall the definition of $c_{(t,n)}(\cdot)$, $\beta_{(T+HL,N)}^*$ and $\hat{\beta}_{(T+tL,N)}$ from Section 3.2. We define regret as,

$$\text{regret} := \sum_{n=1}^N \sum_{t=1}^H [c_{(T+tL,n)}(\hat{\beta}_{(T+tL,n)}) - c_{(T+tL,n)}(\beta_{(T+HL,N)}^*)].$$

Interpretation. Plugging in the definition of $c_{(t,n)}(\cdot)$ we can re-write regret as follows,

$$\begin{aligned} \text{regret} = \sum_{n=1}^N \sum_{t=1}^H & \left\{ [X_n(T+tL) - (X_n(T+(t-1)L+1 : T+tL-1))^T \hat{\beta}_{(T+tL,n)}]^2 \right. \\ & \left. - [X_n(T+tL) - (X_n(T+(t-1)L+1 : T+tL-1))^T \beta_{(T+HL,N)}^*]^2 \right\} \end{aligned}$$

Recall from (2) that $\beta_{(T+HL,N)}^*$ is the estimate produced by the offline forecasting version of mSSA in Section 3.1 if one had access to all $(T+HL) \times N$ data points. Hence, $\sum_{n=1}^N \sum_{t=1}^H c_{(T+tL,n)}(\beta_{(T+HL,N)}^*)$ is the observed *empirical error* of the offline forecasting algorithm if one got all the data in batch. In contrast, $\hat{\beta}_{(T+tL,n)}$ for $(t,n) \in [H] \times [N]$ are the online linear model estimates produced by online-mSSA at each time step *only using* data available till $(T+tL, n)$. Hence, $\sum_{n=1}^N \sum_{t=1}^H c_{(T+tL,n)}(\hat{\beta}_{(T+tL,n)})$ is the observed empirical error using the online estimates produced via online-mSSA. Ideally what one would like to show is that the average difference in empirical error of online-mSSA and that of

⁸Note that M_L^g contains entries of the latent time series for multiples of L , i.e., $\{L, 2L, \dots, T\}$. This can be addressed simply creating L different forecasting models, for $L+i$, for $i \in \{0, 1, \dots, L-1\}$. The corresponding algorithm and theoretical results remain identical. However, this is likely a limitation of our analysis technique and is irrelevant in practice as evidenced in our experiments.

the offline forecasting version of mSSA vanishes as we collect more measurements, i.e., $\frac{1}{NH}$ regret goes to 0 as N and H increase. This is exactly what we establish in Theorem 4.3 and Corollary 4.1.

4.2 mSSA Mean Estimation - Finite Sample Analysis

Rank, Singular Values of $\mathbf{M}_{(lr)}^f$. Recall the definition of $\mathbf{M}_{(lr)}^f$ from Proposition 2.6. Denote rank of $\mathbf{M}_{(lr)}^f$ as r . For $i \in [r]$, let τ_i denote the i -th singular value of $\mathbf{M}_{(lr)}^f$ ordered by magnitude.

PROPERTY 4.1 (WELL-BALANCED SPECTRA). *The non-zero singular values, $\tau_i^{(1)}$, of $\mathbf{M}_{(lr)}^f$ are well-balanced, i.e., $(\tau_i^{(1)})^2 = \Theta(TN/r)$.*

Interpretation. A natural setting in which Property 4.1 holds is the entries of $\mathbf{M}_{(lr)}^f$ are $\Theta(1)$, and the non-zero singular values of $\mathbf{M}_{(lr)}^f$ satisfy $s_i^2 = \Theta(\zeta)$ for some ζ . Then, $Cr\zeta = \|\mathbf{M}_{(lr)}^f\|_F^2 = \Theta(TN)$ for some constant C , i.e., $(\tau_i^{(1)})^2 = \Theta(TN/r)$.

THEOREM 4.1 (mSSA MEAN ESTIMATION: IMPUTATION). *Let Properties 2.1, 2.2, 2.3, 2.4 and 4.1 hold. Let $\rho \geq C \frac{\log(L\bar{P})}{L\bar{P}}$ for absolute constant $C > 0$, $T \geq N$, $\bar{P} = L$, and $\text{rank}(\widehat{\mathbf{M}}^f) = r$. Let C_1 be a term that only depends polynomially on Γ_1 , Γ_2 . Then,*

$$\text{MSE}(\mathbf{M}^f, \widehat{\mathbf{M}}^{f(\text{Impute})}) \leq C_1 \gamma^2 \frac{R^3 G_{\max}}{\rho^4} \left(\frac{1}{\sqrt{TN}} + (\epsilon_{\max})^2 \right) \log(\bar{P}).$$

THEOREM 4.2 (mSSA MEAN ESTIMATION: FORECASTING). *Let conditions of Theorem 4.1 hold. Then,*

$$\text{MSE}(\mathbf{M}^f, \widehat{\mathbf{M}}^{f(\text{Forecast})}) \leq C_1 \gamma^4 \frac{R^5 (G_{\max})^3}{\rho^5} \left(\frac{1}{\sqrt{TN}} + (\epsilon_{\max})^2 \right) \log(\bar{P}).$$

Interpretation. The mSSA imputation and (in-sample) forecasting error bounds in Theorems 4.1 and 4.2 scale as, $O((1/\sqrt{NT}) + (\epsilon_{\max})^2)$. In both results the bound is dominated by the error introduced in Step 2 of the respective algorithms, i.e., the SVT step in Section 3.1. It is straightforward to verify that for the time series dynamics listed in Section 2.2, the approximation error term vanishes as we collect more data. The assumption $\text{rank}(\widehat{\mathbf{M}}^f) = r$, requires that the number of principal components are chosen correctly, i.e., is equal to the (approximate) rank of the stacked Page matrix. In Theorem G.1 in Appendix G, we generalize the above results to the setting where the number of principal components is misspecified, i.e., $\text{rank}(\widehat{\mathbf{M}}^f) \neq r$.

Technical Innovations. The key technical challenge in proving Theorem 4.1 is proving that the singular value thresholding step (i.e., Step 2 of the imputation algorithm) outputs $\widehat{\mathbf{M}}^{f(\text{Impute})}$ which is consistent even when the covariate matrix is well-approximated only in an entry-wise sense by a low-rank matrix (see Lemma E.1). [2] establishes the effectiveness of singular value thresholding only when the covariate matrix is well-approximated in operator norm by a low-rank matrix; *hence, the existing bound in [2] on operator norm error could diverge even if the entry-wise error is diminishing*. To see this, note that for a matrix $\mathbf{A} \in \mathbb{R}^{n \times p}$ where each entry is identical, $\frac{1}{\sqrt{n}} \|\mathbf{A}\| = \sqrt{p} \|\mathbf{A}\|_{\max}$; hence, $\frac{1}{\sqrt{n}} \|\mathbf{A}\|$ will diverge if $\|\mathbf{A}\|_{\max} \gg \frac{1}{\sqrt{p}}$.

The key technical challenge in proving Theorem 4.2 is establishing that when \mathbf{M}^f is approximately low-rank, an approximate linear relationship between $\widehat{\mathbf{M}}^f$ and \mathbf{M}_L^f exists. However it is not guaranteed that such a relationship holds even for an extremely low-rank matrix – to see this, note can easily construct a rank 2 matrix with n rows where the last row is orthogonal to the subspace

spanned by the sub-matrix induced by the first $n - 1$ rows. Thus we have to exploit the particular Page matrix structure in \mathbf{M}^f to prove that an approximate linear relationship between $\bar{\mathbf{M}}^f$ and \mathbf{M}_L^f exists. This is what we do in Proposition G.1. Proving such a linear relationship holds is what motivates fitting a linear model in Step 3 of the forecasting algorithm in Section 3.1.

4.3 mSSA Forecasting (Online Variant) - Regret Analysis

Additional Necessary Notation. We follow the same notation as in Section 3.2; recall the definitions of $Z_{(t,n)}^X$, $\bar{Z}_{(t,n)}^X$, $[Z_{(t,n)}^X]_L$ and $\Omega_{(t,n)}^k$ for $k \in [L-1]$. Let $v_{(t,n)}^1, \dots, v_{(t,n)}^k$ be an orthonormal basis of $\Omega_{(t,n)}^k$ and $v_{(t,n)}^{k+1}, \dots, v_{(t,n)}^{L-1}$ be additional orthonormal vectors to form a complete basis of \mathbb{R}^{L-1} . Let $Z_{(t,n,j)} := [\bar{Z}_{(t,n)}^X]_{\cdot,j}$. Define $a_{(t,n,j)} \in \mathbb{R}^{L-1}$ as $Z_{(t,n,j)} = \sum_{i=1}^{L-1} a_{(t,n,j)}^i v_{(t,n)}^i$.

Define $\mathbf{M}_{(t,n)}^f$, $\bar{\mathbf{M}}_{(t,n)}^f$, $[\mathbf{M}_{(t,n)}^f]_L$ and $\bar{\Omega}_{(t,n)}^k$, for $k \in [L-1]$ analogously to above, but now with respect to the underlying latent time series $f_n(t)$ instead of $X_n(t)$ (recall $\mathbb{E}[X_n(t)] = f_n(t)$). Let $\tau_{(t,n)}^1, \dots, \tau_{(t,n)}^k$ be the first k singular values of $\bar{\mathbf{M}}_{(t,n)}^f$. For a linear subspace defined by Ω , let P_Ω be the associated projection operator (or matrix).

THEOREM 4.3 (ONLINE mSSA: REGRET ANALYSIS). Recall $T = L \times P$. Let Properties 2.1, 2.2, 2.3 and 2.4 hold. Let C_3 be a term that depends only polynomially on Γ_1 , Γ_2 , R , G_{\max} and γ . Further, for $n \in [N]$, $t \in [H+1]$, for some $\epsilon_1, \epsilon_2 \in (0, 1)$ and some $k \in [L-1]$, let the following hold:

- A.1 $P_{\bar{\Omega}_{(T+tL,n)}^k} = P_{\bar{\Omega}_{(T+HL,N)}^k}$;
- A.2 $\tau_{(T+tL,n)}^k = \Omega\left(\sqrt{\frac{LNP}{k}}\right)$, $\tau_{(T+tL,n)}^{k+1} = 0$;
- A.3 $L = P^{1-\epsilon_1}$, $H = P^{1-\epsilon_2}$;
- A.4 $\|\hat{\beta}_{(T+tL,n)}\|_2 \leq C_3 k$, for $\hat{\beta}_{(T+tL,n)} \in \Omega_{(t,n)}^k$;
- A.5 $\max_{i,j} |a_{(T+tL,n,j)}^i| \leq C_3 \sqrt{\frac{L}{k}}$;
- A.6 $|X_n(T+tL)| \leq C_3$.

Picking $\delta = \frac{1}{L} \sqrt{\frac{1}{NH} + \sqrt{\frac{H}{P}}}$, we get that with probability at least $1 - 1/(NT)$,

$$\frac{1}{NH} \text{regret} \leq C_3 k^{2.5} \sqrt{\left(\frac{P^{1-2\epsilon_1+\epsilon_2}}{N} + P^{2-2\epsilon_1-0.5\epsilon_2}\right)}.$$

COROLLARY 4.1. Let conditions of Theorem 4.3 hold. Pick $\epsilon_1 = 0.86$, $\epsilon_2 = 0.67$. Then, with probability at least $1 - 1/(NT)$,

$$\frac{1}{NH} \text{regret} \leq C_3 k^{2.5} \frac{1}{\sqrt{NT^{0.04}}}.$$

Interpretation of Assumptions.

- A.1 This is the key assumption made. In essence, it requires that T is large enough such that the latent k -dimensional subspaces of the stacked Page matrix induced by the time series, f i.e., $\bar{\mathbf{M}}_{(t,n)}^f$ are no longer varying. An interpretation of this assumption is that for matrix-factorization based time series algorithms, such as mSSA, this serves as an analog of the i.i.d assumption of the underlying generating process that is made in classical generalization error analysis (e.g. Rademacher analysis). We stress however that this does not mean that $\Omega_{(T+tL,n)}^k$ is not varying.
- A.2 This is analogous to Property 4.1 holding.

- A.3 This requires that the number of steps, H , that we do “online” forecasting for grows sub-linearly in the number of observations during the “offline” phase of mSSA; the same goes for L , which is intuitively the allowed model complexity.
- A.4 This is a standard boundedness assumption i.e., the linear model should not scale larger than the dimension of the subspace we project onto.
- A.5 This is to ensure consistency with Assumption A.2, i.e., the coefficients, $a_{(\cdot)}$ we get after projection onto $\bar{\Omega}_{(T+tL,n)}^k$ are well-balanced.
- A.6 This can easily be verified to hold in high-probability using standard concentration inequalities for sub-Gaussian random variables.

Technical Innovation. Note the key technical difficultly of our setting is that the subspaces $\Omega_{(T+tL,n)}^k$ are varying over time (due to noise in the observations), a setting not studied closely in the online learning literature. This is what leads to a sub-optimal rate of regret of $N^{-1/2}T^{-0.04}$. Improving this rate for our more involved setting, and seeing whether one can achieve the optimal rate of $(NT)^{-1/2}$ that one gets in traditional online learning without time-varying constraints is an important future research direction.

5 EXPERIMENTS

We detail the experimental setup and the datasets used to produce the results in Table 2. Section 5.1 describes in detail the datasets used, the experimental setup, and finally the results for the mean imputation and forecasting experiments. Section 5.2 provides details about the parameters and implementations used for all algorithms used in the experiments.

Note that in all experiments, Normalized Root Mean Squared Error (NRMSE) is used as an accuracy metric. In particular, time series is normalized to have zero mean and unit variance before calculating the RMSE. We use this metric as it weighs the error on each time series equally.

5.1 Mean Estimation

5.1.1 Datasets.

In the mean estimation experiments, we use three real-world datasets and one synthetic dataset. The description and preprocessing we do on these four datasets are as follows:

Electricity Dataset. This is a public dataset obtained from the UCI repository which shows the 15-minutes electricity load of 370 household ([19]). As was done in [26], [18], [17], we aggregate the data into hourly intervals and use the first 25968 time-points for training. The goal here is to do 24-hour ahead forecasts for the next seven days (i.e. 24-step ahead forecast).

Traffic Dataset. This public dataset obtained from the UCI repository shows the occupancy rate of traffic lanes in San Francisco ([19]). The data is sampled every 15 minutes but to be consistent with previous work in [26], [18], we aggregate the data into hourly data and use the first 10392 time-points for training. The goal here is to do 24-hour ahead forecasts for the next seven days (i.e. 24-step ahead forecast).

Financial Dataset. This dataset is obtained from Wharton Research Data Services (WRDS) and contains the average daily stocks prices of 839 companies from October 2004 till November 2019 [24]. The datasets were preprocessed to remove stocks with any null values, or those with an average price below 30\$ across the aforementioned period. This was simply done to constrain the number of time series for ease of experimentation and we end up with 839 time series (i.e. stock prices of listed companies) each with 3993 readings of daily stock prices. For forecasting, we

consider the predicting the 180 time-points ahead one point at a time, and we train on the first 3813 time points. The goal here is to do one-day ahead forecasts for the next 180 days (i.e. 1-step ahead forecast). We choose to do so as this is a standard goal in finance.

Synthetic Dataset. We generate the observation tensor $X \in \mathbb{R}^{n \times m \times T}$ by first randomly generating the two vectors $U \in \mathbb{R}^n = [u_1, \dots, u_n]$ and $V \in \mathbb{R}^m = [v_1, \dots, v_n]$. Then, we generate r mixtures of harmonics where each mixture $g_k(t), k \in [r]$, is generated as: $g_k(t) = \sum_{h=1}^4 \alpha_h \cos(\omega_h t/T)$ where the parameters are selected randomly such that $\alpha_h \in [-1, 10]$ and $\omega_h \in [1, 1000]$. Then each value in the observation tensor is constructed as follows:

$$X_{i,j}(t) = \sum_{k=1}^r u_i v_j g_k(t)$$

where r is the tensor rank, $i \in [n]$, $j \in [m]$. In our experiment, we select $n = 20$, $m = 20$, $T = 15000$, and $r = 4$. This gives us 400 time series each with 15000 observations. In the forecasting experiments, we use the first 14000 points for training. The goal here is to do 10-step ahead forecasts for the final 1000 points.

5.1.2 Mean Imputation.

Setup. We test the robustness of the imputation performance by adding two sources of corruption to the data - varying the percentage of observed values and varying the amount of noise we perturb the observations by. We test imputation performance by how accurately we recover missing values. We compare the performance of mSSA with TRMF, a method which achieves state-of-the-art imputation performance. Further, to analyze the added benefit of exploiting the spatial structure in a multivariate time series using mSSA, we compare with the SSA variant introduced in [1]. See details about the implementation of, and parameters used for TRMF and SSA in Section 5.2.

Results. Figures 1 (a)-(d) show the imputation error in the aforementioned datasets as we vary the fraction of missing values, while Figures 1 (e)-(h) show the imputation error as we vary σ , the standard deviation of the gaussian noise. We see that as we vary the fraction of missing values and noise levels, mSSA outperforms both TRMF and SSA in $\sim 80\%$ of experiments run. It is noteworthy the large empirical gain in mSSA over SSA, giving credence to the spatio-temporal model we introduce. The average NRMSE across all experiments for each dataset is reported in Table 2, where mSSA outperforms every other method across all datasets.

5.1.3 Mean Forecasting.

Setup. We test the forecasting accuracy of the proposed mSSA against several state-of-the-art algorithms. For each dataset, we split the data into training and testing datasets as outlined in Section 5.1.1. As was done in the imputation experiments, we vary the conditions of the datasets by varying the percentage of observed values and the noise levels.

We compare against several methods, namely: (i) SSA, specifically the variant introduced in [1]; (ii) LSTM, available through the Keras library (a standard deep learning library); (iii) DeepAR, a state-of-the-art, deep learning method designed for multivariate time series [17]; (iv) TRMF, a matrix factorization approach with temporal regularization hat has gained in popularity recently [26]; (v) Prophet, Facebook's time series forecasting library [7]. Refer to Section 5.2 for details about the implementations of these algorithms and the selected hyper-parameters.

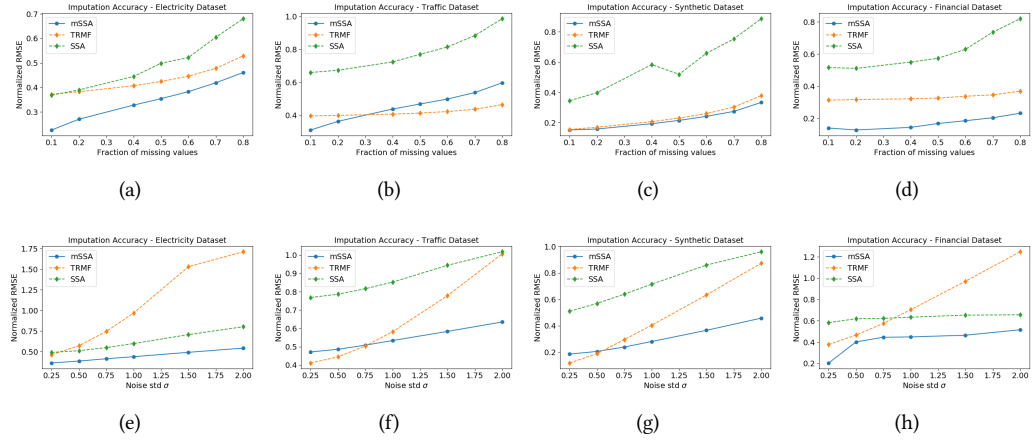


Fig. 1. mSSA vs. TRMF vs. SSA - imputation performance on standard multivariate time series benchmarks and synthetic data. Figures 1 (a)-(d) shows imputation accuracy of mSSA, TRMF and SSA as we vary the fraction of missing values; Figures 1 (e)-(h) shows imputation accuracy as we vary the noise level (and with 50% of values missing).

Results. Figures 2 (a)-(d) show the forecasting accuracy of mSSA vs. these methods in the aforementioned datasets as we vary the fraction of missing values, while Figures 2 (e)-(h) shows the forecasting accuracy as we vary the standard deviation of the added gaussian noise. We see that as we vary the fraction of missing values and noise levels, mSSA is the best or comparable to the best performing method in $\sim 80\%$ of experiments. In terms of the average NRMSE across all experiments, we find that mSSA outperforms every other method across all datasets except for the traffic dataset (see Table 2).

5.2 Algorithms Parameters and Settings

In this section, we describe the algorithms used throughout the experiments in more detail, as well as describing the hyper-parameters/implementation used for each method.

mSSA & SSA. Note that since the SSA's variant described in [1] is a special case of our proposed mSSA algorithm, we use our mSSA's implementation to perform SSA experiments, however without “stacking” the various Page matrices induced by each time series. For all experiments we choose k , the number of retained singular values, in a data-driven manner. Specifically, we choose k based on the thresholding procedure outlined in [8], where the threshold is determined by the median of the singular values and the shape of the matrix. Finally, as guided by our theoretical results to create an approximately ‘square’ Page matrix (i.e. $L = \bar{P}$), we choose $L = 1000$ (100 for SSA) for all experiments other than the financial dataset where we choose $L = 500$ (50 for SSA).

DeepAR. We use the default parameters of “DeepAREstimator” algorithm provided by the GluonTS package.

LSTM. Across all datasets, we use a LSTM network with three hidden layers each, with 45 neurons per layer, as is done in [18]. We use the Keras implementation of LSTM.

Prophet. We used Prophet's Python library with the default parameters selected [7].

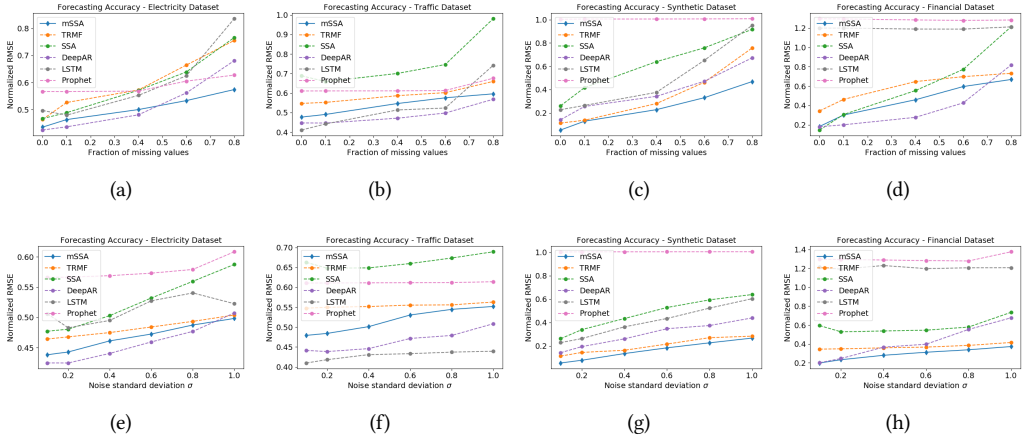


Fig. 2. mSSA forecasting performance on standard multivariate time series benchmark is competitive with/outperforming industry standard methods as we vary the number of missing data and noise level. Figures 2 (a)-(d) shows the forecasting accuracy of all methods on the four datasets with varying fraction of missing values; Figures 2 (e)-(h) shows the forecasting accuracy on the same four datasets with varying noise level.

TRMF. We use the implementation provided by the authors in the Github repository associated with the paper ([26]). For the parameter k , which represent the chosen rank for the $T \times N$ Time series matrix, we use $k = 60$ for the electricity dataset, $k = 40$ for the traffic dataset, $k = 20$ for the financial and synthetic datasets. The lag indices include the last day and the same weekday in last week for the traffic and electricity data. For the financial and synthetic dataset, the lag indices include the last 30 points.

6 CONCLUSION

In this work, we provide theoretical justification of mSSA, a method heavily used in practice but with limited theoretical understanding. Using a spatio-temporal factor model that we introduce, we argue the finite sample error for imputation and forecasting scales as $1/\sqrt{NT}$ for N time series with observations over T time steps. The key technical contributions are: (a) establishing the stacked Page matrix, the core data representation in mSSA, is approximately low-rank for a large model class – in doing so, we establish a ‘calculus’ for approximate low-rank models for which mSSA is effective; (b) advancing the finite-sample analysis of PCR to obtain tight imputation and forecasting results for mSSA; (c) introducing an OCO framework to quantify the out-of-sample performance for time series methods as traditional generalization frameworks such as Rademacher analysis do not apply in our setting; (d) extending the theory of OCO to allow for a time varying decision set.

As an important direction for future research, it is worth exploring whether our regret bounds can be made tighter and/or whether we can produce lower bounds for the out-of-sample performance of mSSA and time series methods more broadly. On a related note, we also believe it is worth exploring the sample complexity gains by using a variant of mSSA that utilizes higher-dimensional ‘tensor’ structure induced by the Page Matrices of multiple time series rather than “stacking” them up as a larger matrix.

REFERENCES

- [1] Anish Agarwal, Muhammad Jehangir Amjad, Devavrat Shah, and Dennis Shen. 2018. Model Agnostic Time Series Analysis via Matrix Estimation. *Proceedings of the ACM on Measurement and Analysis of Computing Systems* 2, 3 (2018), 40.
- [2] Anish Agarwal, Devavrat Shah, Dennis Shen, and Dogyoon Song. 2019. On robustness of principal component regression. In *Advances in Neural Information Processing Systems*. 9889–9900.
- [3] Peter L. Bartlett and Shahar Mendelson. 2003. Rademacher and Gaussian Complexities: Risk Bounds and Structural Results. *J. Mach. Learn. Res.* 3 (March 2003), 463–482. <http://dl.acm.org/citation.cfm?id=944919.944944>
- [4] Sergei Bernstein. 1946. *The Theory of Probabilities*. Gasteizdat Publishing House.
- [5] François Chollet. 2015. keras. <https://github.com/fchollet/keras>.
- [6] Chandler Davis and William Morton Kahan. 1970. The rotation of eigenvectors by a perturbation. III. *SIAM J. Numer. Anal.* 7, 1 (1970), 1–46.
- [7] Facebook. [n.d.]. Prophet. <https://facebook.github.io/prophet/>. Online; accessed 25 February 2020.
- [8] Matan Gavish and David L Donoho. 2014. The optimal hard threshold for singular values is $4/\sqrt{3}$. *IEEE Transactions on Information Theory* 60, 8 (2014), 5040–5053.
- [9] Nina Golyandina, Vladimir Nekrutkin, and Anatoly A Zhigljavsky. 2001. *Analysis of time series structure: SSA and related techniques*. Chapman and Hall/CRC.
- [10] Loukas Grafakos. 2008. *Classical Fourier analysis*. Vol. 2. Springer.
- [11] Hossein Hassani, Saeed Heravi, and Anatoly Zhigljavsky. 2013. Forecasting UK industrial production with multivariate singular spectrum analysis. *Journal of Forecasting* 32, 5 (2013), 395–408.
- [12] Hossein Hassani and Rahim Mahmoudvand. 2013. Multivariate singular spectrum analysis: A general view and new vector forecasting approach. *International Journal of Energy and Statistics* 1, 01 (2013), 55–83.
- [13] Elad Hazan. 2019. Introduction to Online Convex Optimization. arXiv:1909.05207 [cs.LG]
- [14] Vicente Oropesa and Mauricio Sacchi. 2011. Simultaneous seismic data denoising and reconstruction via multichannel singular spectrum analysis. *Geophysics* 76, 3 (2011), V25–V32.
- [15] Alexander Rakhlin, Karthik Sridharan, and Ambuj Tewari. 2015. Online Learning via Sequential Complexities. *J. Mach. Learn. Res.* 16, 1 (Jan. 2015), 155–186.
- [16] Nikhil Rao, Hsiang-Fu Yu, Pradeep K Ravikumar, and Inderjit S Dhillon. 2015. Collaborative Filtering with Graph Information: Consistency and Scalable Methods. In *Advances in Neural Information Processing Systems* 28, C. Cortes, N. D. Lawrence, D. D. Lee, M. Sugiyama, and R. Garnett (Eds.). Curran Associates, Inc., 2107–2115. <http://papers.nips.cc/paper/5938-collaborative-filtering-with-graph-information-consistency-and-scalable-methods.pdf>
- [17] David Salinas, Valentin Flunkert, Jan Gasthaus, and Tim Januschowski. 2019. DeepAR: Probabilistic forecasting with autoregressive recurrent networks. *International Journal of Forecasting* (2019).
- [18] Rajat Sen, Hsiang-Fu Yu, and Inderjit S Dhillon. 2019. Think globally, act locally: A deep neural network approach to high-dimensional time series forecasting. In *Advances in Neural Information Processing Systems*. 4838–4847.
- [19] Artur Trindade. [n.d.]. UCI Machine Learning Repository - Individual Household Electric Power Consumption Data Set. ([n. d.]). <https://archive.ics.uci.edu/ml/datasets/ElectricityLoadDiagrams20112014>
- [20] Roman Vershynin. 2010. Introduction to the non-asymptotic analysis of random matrices. *arXiv preprint arXiv:1011.3027* (2010).
- [21] Larry Wasserman. 2006. *All of nonparametric statistics*. Springer.
- [22] Per-Åke Wedin. 1972. Perturbation bounds in connection with singular value decomposition. *BIT Numerical Mathematics* 12, 1 (1972), 99–111.
- [23] Kevin W Wilson, Bhiksha Raj, and Paris Smaragdis. 2008. Regularized non-negative matrix factorization with temporal dependencies for speech denoising. In *Ninth Annual Conference of the International Speech Communication Association*.
- [24] WRDS. [n.d.]. The Trade and Quote (TAQ) database. ([n. d.]). <https://wrds-www.wharton.upenn.edu/pages/support/data-overview/wrds-overview-taq/>
- [25] Jiaming Xu. 2017. Rates of convergence of spectral methods for graphon estimation. *arXiv preprint arXiv:1709.03183* (2017).
- [26] Hsiang-Fu Yu, Nikhil Rao, and Inderjit S Dhillon. 2016. Temporal regularized matrix factorization for high-dimensional time series prediction. In *Advances in neural information processing systems*. 847–855.

Overview of Appendix. The supplementary material provides detailed technical proofs of the results stated in the main body. Appendices A and B provide supporting technical proofs for the fundamental representation results that forms the basis of our results. Appendices C, D and E provide supporting notation and results that are utilized in Appendices F and G, which provide proof of our imputation and forecasting analysis respectively. Finally, Section H provides proofs associated with regret analysis.

A PROOFS - (G, ϵ) -HANKEL REPRESENTABILITY OF DIFFERENT TIME SERIES DYNAMICS

A.1 Proof of Proposition 2.1

PROOF. Noting that for any two matrices A and B , it is the case that $\text{rank}(A + B) \leq \text{rank}(A) + \text{rank}(B)$ and $\text{rank}(A \circ B) \leq \text{rank}(A)\text{rank}(B)$ (where \circ denotes the Hadamard product), completes the proof. \square

A.2 Proof of Proposition 2.2

PROOF. Proof is immediate from Definitions 2.1 and 2.2. \square

A.3 Proof of Proposition 2.4

A.3.1 Helper Lemmas for Proposition 2.4. We begin by stating some classic results from Fourier Analysis. To do so, we introduce some notation.

$C[0, R']$ and $L^2[0, R']$ functions. $C[0, R']$ is the set of real-valued, continuous functions defined on $[0, R']$. $L^2[0, R']$ is the set of square integrable functions, i.e. $\int_0^{R'} f^2(t)dt \leq \infty$

Inner Product of functions in $L^2[0, R']$. $L^2[0, R']$ is an inner product space endowed with inner product defined as $\langle f, g \rangle := \frac{1}{R'} \int_0^{R'} f(t)g(t)dt$, and associated norm as $\|f\| := \sqrt{\frac{1}{R'} \int_0^{R'} f^2(t)dt}$.

Fourier Representation of functions in $L^2[0, R']$. For a function, f , in $L^2[0, R']$, define S_G as follows

$$S_G(t) = a_0 + \sum_{n=1}^G (a_n \cos(2\pi nt/R') + b_n \sin(2\pi nt/R')) \quad (3)$$

where for $n \in [N]$ (a_0, a_n, b_n are called the Fourier coefficients of f),

$$\begin{aligned} a_0 &:= \langle f, 1 \rangle = \frac{1}{R'} \int_0^{R'} f(t)dt, \\ a_n &:= \langle f, \cos(2\pi nt/R') \rangle = \frac{1}{R'} \int_0^{R'} f(t) \cos(2\pi nt/R')dt, \\ b_n &:= \langle f, \sin(2\pi nt/R') \rangle = \frac{1}{R'} \int_0^{R'} f(t) \sin(2\pi nt/R')dt. \end{aligned}$$

We now state a classic result from Fourier analysis.

THEOREM A.1 ([10]). *If $f \in C_{per-R}^k$, for $k \geq 1$, then S_G converges pointwise to f , i.e., for all $t \in R'$*

$$\lim_{G \rightarrow \infty} S_G(t) \rightarrow f(t).$$

We next show that if f is k -times differentiable, then its Fourier coefficients decay rapidly. Precisely,

LEMMA A.1. If $f \in C_{per-R'}^k$, for $k \geq 1$, then for $k' \in [k]$, the Fourier coefficients of $f^{(k')}$, the k' -th derivative of f , are defined as

$$a_0^{(k)} = a_0, \quad a_n^{(k)} = -\left(\frac{2\pi n}{R'}\right)b_n^{(k-1)}, \quad b_n^{(k)} = \left(\frac{2\pi n}{R'}\right)a_n^{(k-1)}$$

PROOF. We show it for $a_n^{(1)}$. Extension to $a_n^{(k')}$ for $k' \in [k]$ follows by induction in a straightforward manner.

$$\begin{aligned} a_n^{(1)} &= \langle f^{(1)}, \cos(2\pi nt/R') \rangle = \frac{1}{R'} \int_0^{R'} f^{(1)}(t) \cos(2\pi nt/R') dt \\ &\stackrel{(a)}{=} \frac{1}{R'} \left(\left[f(t) \cos(2\pi nt/R') \right]_0^{R'} - \frac{2\pi n}{R'} \left[\int_0^{R'} f(t) \sin(2\pi nt/R') \right]_0^{R'} \right) \\ &= -\left(\frac{2\pi n}{R'}\right)b_n^{(0)}. \end{aligned}$$

(a) follows by integration by parts. The identity for $b_n^{(k')}$ follows in a similar fashion, as does it for $a_0^{(k)}$. \square

A.3.2 Completing Proof of Proposition 2.4.

PROOF. For $G \in \mathbb{N}$, let S_G be defined as in (3). Then for $t \in \mathbb{R}$

$$\begin{aligned} |f(t) - S_G(t)| &\stackrel{(a)}{=} \left| \sum_{n=G+1}^{\infty} (a_n \cos(2\pi nt/R') + b_n \sin(2\pi nt/R')) \right| \\ &\leq \sum_{n=G+1}^{\infty} |a_n| + |b_n| \\ &\stackrel{(b)}{\leq} \sum_{n=G+1}^{\infty} \left(\frac{R'}{2\pi n}\right)^k (|a_n^{(k)}| + |b_n^{(k)}|) \\ &\stackrel{(c)}{\leq} \sqrt{2} \left(\frac{R'}{2\pi}\right)^k \sqrt{\sum_{n=G+1}^{\infty} \left(\frac{1}{n}\right)^{2k}} \sqrt{\sum_{n=G+1}^{\infty} (|a_n^{(k)}|^2 + |b_n^{(k)}|^2)} \\ &\leq \sqrt{2} \left(\frac{R'}{2\pi}\right)^k \frac{1}{G^{k-0.5}} \sqrt{\sum_{n=G+1}^{\infty} (|a_n^{(k)}|^2 + |b_n^{(k)}|^2)} \\ &\stackrel{(d)}{\leq} \sqrt{2} \left(\frac{R'}{2\pi}\right)^k \frac{\|f^k\|}{G^{k-0.5}} \\ &= C(k, R') \frac{\|f^k\|}{G^{k-0.5}} \end{aligned}$$

where $C(k, R')$ is a constant that depends only on k and R' ; (a) follows from Theorem A.1; (b) follows from Lemma A.1; (c) follows from Cauchy-Schwarz inequality; (d) follows from Bessel's inequality.

Hence S_G , a sum of $2G$ harmonics, gives an uniform approximation to f with error at most $C(k, R') \frac{\|f^k\|}{G^{k-0.5}}$. Noting $2G$ harmonics can be represented by an order- $4G$ LRF (by Proposition 2.3) completes the proof. \square

A.4 Proof of Proposition 2.5

This analysis is closely adapted from [25] and is stated for completeness.

PROOF. Step 1: Partitioning the space $[0, 1]^K$. Let \mathcal{E} denote a partition of the cube $[0, 1]^K$ into a finite number (denoted by $|\mathcal{E}|$) of cubes Δ . Let $\ell \in \mathbb{N}$. We say $P_{\mathcal{E}, \ell} : [0, 1]^K \rightarrow \mathbb{R}$ is a piecewise polynomial of degree ℓ if

$$P_{\mathcal{E}, \ell}(\theta) = \sum_{\Delta \in \mathcal{E}} P_{\Delta, \ell}(\theta) \mathbb{1}(\theta \in \Delta), \quad (4)$$

where $P_{\Delta, \ell}(\theta) : [0, 1]^K \rightarrow \mathbb{R}$ denotes a polynomial of degree at most ℓ .

It suffices to consider an equal partition of $[0, 1]^K$. More precisely, for any $k \in \mathbb{N}$, we partition the set $[0, 1]$ into $1/k$ half-open intervals of length $1/k$, i.e., $[0, 1] = \bigcup_{i=1}^k [(i-1)/k, i/k]$. It follows that $[0, 1]^K$ can be partitioned into k^K cubes of forms $\bigotimes_{j=1}^K [(i_j-1)/k, i_j/k]$ with $i_j \in [k]$. Let \mathcal{E}_k be such a partition with I_1, I_2, \dots, I_{k^K} denoting all such cubes and $z_1, z_2, \dots, z_{k^K} \in \mathbb{R}^K$ denoting the centers of those cubes.

Step 2: Taylor Expansion of $g(\cdot, \omega_s)$. For Step 2 of the proof, to reduce notational overload, we suppress dependence of ω_s on g , we abuse notation by using $g(\cdot) = g(\cdot, \omega_s)$.

For every I_i with $1 \leq i \leq k^K$, define $P_{I_i, \ell}(x)$ as the degree- ℓ Taylor's series expansion of $g(x)$ at point z_i :

$$P_{I_i, \ell}(x) = \sum_{\kappa: |\kappa| \leq \ell} \frac{1}{\kappa!} (x - z_i)^\kappa \nabla_\kappa g(z_i), \quad (5)$$

where $\kappa = (\kappa_1, \dots, \kappa_d)$ is a multi-index with $\kappa! = \prod_{i=1}^K \kappa_i!$, and $\nabla_\kappa g(z_i)$ is the partial derivative defined in Section 2.2.4. Note similar to g , $P_{I_i, \ell}(x)$ really refers to $P_{I_i, \ell}(x, \omega_s)$.

Now we define a degree- ℓ piecewise polynomial as in (4), i.e.,

$$P_{\mathcal{E}_k, \ell}(x) = \sum_{i=1}^{k^K} P_{I_i, \ell}(x) \mathbb{1}(x \in I_i). \quad (6)$$

For the remainder of the proof, let $\ell = \lfloor \alpha \rfloor$ (recall $\lfloor \alpha \rfloor$ refers to the largest integer strictly larger than α).

Since $f \in \mathcal{H}(\alpha, L)$, it follows that

$$\begin{aligned}
\sup_{x \in \mathcal{X}} |g(x) - P_{\mathcal{E}_k, \ell}(x)| &= \sup_{1 \leq i \leq k^K} \sup_{x \in I_i} |g(x) - P_{I_i, \ell}(x)| \\
&\stackrel{(a)}{=} \sup_{1 \leq i \leq k^K} \sup_{x \in I_i} \left| \sum_{\kappa: |\kappa| \leq \ell-1} \frac{\nabla_\kappa g(z_i)}{\kappa!} (x - z_i)^\kappa + \sum_{\kappa: |\kappa| = \ell} \frac{\nabla_\kappa g(z'_i)}{\kappa!} (x - z_i)^\ell - P_{\mathcal{E}_k, \ell}(x) \right| \\
&= \sup_{1 \leq i \leq k^K} \sup_{x \in I_i} \left| \sum_{\kappa: |\kappa| \leq \ell-1} \frac{\nabla_\kappa g(z_i)}{\kappa!} (x - z_i)^\ell \pm \sum_{\kappa: |\kappa| = \ell} \frac{\nabla_\kappa g(z_i)}{\kappa!} (x - z_i)^\ell + \sum_{\kappa: |\kappa| = \ell} \frac{\nabla_\kappa g(z'_i)}{\kappa!} (x - z_i)^\ell - P_{\mathcal{E}_k, \ell}(x) \right| \\
&= \sup_{1 \leq i \leq k^K} \sup_{x \in I_i} \left| \sum_{\kappa: |\kappa| \leq \ell} \frac{\nabla_\kappa g(z_i)}{\kappa!} (x - z_i)^\ell + \sum_{\kappa: |\kappa| = \ell} \frac{\nabla_\kappa g(z'_i) - \nabla_\kappa g(z_i)}{\kappa!} (x - z_i)^\ell - P_{\mathcal{E}_k, \ell}(x) \right| \\
&= \sup_{1 \leq i \leq k^K} \sup_{x \in I_i} \left| \sum_{\kappa: |\kappa| = \ell} \frac{\nabla_\kappa g(z'_i) - \nabla_\kappa g(z_i)}{\kappa!} (x - z_i)^\ell \right| \\
&\stackrel{(b)}{\leq} \sup_{1 \leq i \leq k^K} \sup_{x \in I_i} \|x - z_i\|_\infty^\ell \sup_{x \in I_i} \sum_{\kappa: |\kappa| = \ell} \frac{1}{\kappa!} |\nabla_\kappa g(z'_i) - \nabla_\kappa g(z_i)| \\
&\stackrel{(c)}{\leq} \mathcal{L} k^{-\alpha}.
\end{aligned}$$

where (a) follows from multivariate's version of Taylor's theorem (and using the Lagrange form for the remainder) and $z'_i \in [0, 1]^K$ is a vector that can be represented as $z_i + cx$ for $c \in (0, 1)$; (b) follows from Holder's inequality; (c) follows from Property 2.5.

Step 3: Construct Low-Rank Approximation of Time Series Hankel Using $P_{\mathcal{E}_k, \ell}(\cdot, \omega_s)$. Recall the Hankel matrix, $\mathbf{H} \in \mathbb{R}^{L \times T}$ induced by the original time series, where $\mathbf{H}_{ts} = g(\theta_t, \omega_s)$, and $g(\cdot, \omega_s) \in \mathcal{H}(\alpha, \mathcal{L})$. We now construct a low-rank approximation of it using $P_{I_i, \ell}(\cdot, \omega_s)$. Define $\mathbf{H}_{(lr)} \in \mathbb{R}^{L \times T}$, where $[\mathbf{H}_{(lr)}]_{(t,s)} = P_{\mathcal{E}_k, \ell}(\theta_t, \omega_s)$.

By Step 2, we have that for all $t \in [L], s \in [T]$,

$$|\mathbf{H}_{ts} - [\mathbf{H}_{(lr)}]_{(t,s)}| \leq \mathcal{L} k^{-\alpha}$$

It remains to bound the rank of $\mathbf{H}_{(lr)}$. Note that since $P_{\mathcal{E}_k, \ell}(\theta_t, \omega_s)$ is a piecewise polynomial of degree $\ell = \lfloor \alpha \rfloor$, it has a decomposition of the form

$$[\mathbf{H}_{(lr)}]_{(t,s)} = P_{\mathcal{E}_k, \ell}(\theta_t, \omega_s) = \sum_{i=1}^{k^K} \langle \Phi(\theta), \beta_{I_i, s} \rangle \mathbb{1}(\theta \in I_i)$$

where the vector

$$\Phi(\theta) = \left(1, \theta_1, \dots, \theta_K, \dots, \theta_1^\ell, \dots, \theta_K^\ell \right)^T,$$

i.e., is the vector of all monomials of degree less than or equal to ℓ . The number of such monomials is easily show to be equal to $C(\alpha, K) := \sum_{i=0}^{\lfloor \alpha \rfloor} \binom{i+K-1}{K-1}$.

Thus the rank of $\mathbf{H}_{(lr)}$ is bounded by $k^K C(\alpha, K)$. Setting $k = \frac{1}{\epsilon}$ completes the proof. \square

B PROOFS - STACKED HANKEL MATRIX IS APPROXIMATELY LOW-RANK

B.1 Helper Lemmas

LEMMA B.1. *Let Property 2.1 hold. Then*

$$\|\mathbf{M}^f\|_{\max} \leq R\Gamma_1\Gamma_2$$

PROOF. Proof is immediate. \square

PROPOSITION B.1. *Let f be a $(G, 0)$ -LRF, then for $s \in \{1, \dots, L\}$, $t \in \{0, P, \dots, (P-1)L\}$, f admits the representation*

$$f(s+t) = \sum_{g=1}^G \alpha_g a_g(s) b_g(t) \quad (7)$$

for some scalars α_g , and functions $a_g : [L] \rightarrow \mathbb{R}$ and $b_g : [P] \rightarrow \mathbb{R}$.

PROOF. Note the page matrix \mathbf{M}^f corresponding to time series f has rank at most G . Thus the singular value decomposition of \mathbf{M}^f has the form, $\mathbf{M}^f = \sum_{g=1}^G \alpha_g a'_g b'_g$ where α_g are the singular values, and $a'_g \in \mathbb{R}^L, b'_g \in \mathbb{R}^N$ are the left and right singular vectors of \mathbf{M}^f respectively. Thus M_{ij}^f has the following form, $M_{ij}^f = f(i + (j-1)L) = \sum_{g=1}^G \alpha_g a'_g(i) b'_g(j)$. Identifying a_g, b_g as a'_g, b'_g respectively completes the proof. \square

PROPOSITION B.2. *Let f be a $(G, 0)$ -Hankel, then for $s \in \{1, \dots, L\}$, $t \in \{0, P, \dots, (P-1)L\}$, f admits the representation*

$$f(s+t) = \sum_{g=1}^G \alpha_g a_g(s) b_g(t) \quad (8)$$

for some scalars α_g , and functions $a_g : [L] \rightarrow \mathbb{R}$ and $b_g : [P] \rightarrow \mathbb{R}$.

PROOF. Identical to that of Proposition B.1. \square

B.2 Proof of Proposition 2.6

PROOF. To reduce notational complexity, we suppress the superscript f for the remainder of the proof. For $l \in [L], k \in [T], n \in [N]$ we have,

$$\begin{aligned} H_{l, [k+(T-L+1) \times (n-1)]} &= f_n(l + (k-1)) \\ &= \sum_{r=1}^R U_{nr} W_r(l + (k-1)) \\ &\stackrel{(a)}{=} \sum_{r=1}^R U_{nr} \left(\sum_{g=1}^{G_r} \alpha_g^r a_g^r(l) b_g^r((k-1)) + \epsilon_r(l + (k-1)) \right) \\ &= \sum_{r=1}^R \sum_{g=1}^{G_r} a_g^r(l) \left[U_{nr} \cdot \alpha_g^r \cdot b_g^r((k-1)) \right] + \sum_{r=1}^R U_{nr} \epsilon_r(l + (k-1)) \end{aligned}$$

where (a) follows from directly from Property 2.2 and Proposition B.2; here $\epsilon_r(l + (k-1)) = [H^{W_r} - H_{(l,r)}^{W_r}]_{(l,k)}$.

$$\left| \sum_{r=1}^R U_{nr} \epsilon_r (l + (k - 1)) \right| \leq \epsilon_{\max} \left| \sum_{r=1}^R U_{nr} \right| \leq R \epsilon_{\max} \Gamma_1$$

This completes the proof. \square

C IMPUTATION AND FORECASTING ERROR ANALYSIS - PROOF NOTATION

C.1 Induced Linear Operator

Consider a matrix $\mathbf{B} \in \mathbb{R}^{N \times p}$ such that $\mathbf{B} = \sum_{i=1}^{N \wedge p} \sigma_i(\mathbf{B}) x_i y_i^T$. Here, $\sigma_i(\mathbf{B})$ are the singular vectors of \mathbf{B} and x_i, y_i are the left and right singular vectors respectively.

Hard Singular Value Thresholding. To that end, given any $\lambda > 0$, we define the map $\text{HSVT}_\lambda : \mathbb{R}^{N \times p} \rightarrow \mathbb{R}^{N \times p}$, which simply shaves off the input matrix's singular values that are below the threshold λ . Precisely,

$$\text{HSVT}_\lambda(\mathbf{B}) = \sum_{i=1}^{N \wedge p} \sigma_i(\mathbf{B}) \mathbb{1}(\sigma_i(\mathbf{B}) \geq \lambda) x_i y_i^T. \quad (9)$$

Induced Linear Operator. With a specific choice of $\lambda \geq 0$, we can define a function $\varphi_\lambda^{\mathbf{B}} : \mathbb{R}^p \rightarrow \mathbb{R}^p$ as follows: for any vector row $w \in \mathbb{R}^p$ (i.e. $w \in \mathbb{R}^{1 \times p}$),

$$\varphi_\lambda^{\mathbf{B}}(w) = \sum_{i=1}^{N \wedge p} \mathbb{1}(\sigma_i(\mathbf{B}) \geq \lambda) y_i y_i^T w^T. \quad (10)$$

Note that $\varphi_\lambda^{\mathbf{B}}$ is a linear operator and it depends on the tuple (\mathbf{B}, λ) ; more precisely, the singular values and the right singular vectors of \mathbf{B} , as well as the threshold λ . If $\lambda = 0$, then we will adopt the shorthand notation: $\varphi^{\mathbf{B}} = \varphi_0^{\mathbf{B}}$.

LEMMA C.1 (LEMMA 35 OF [2]). *Let $\mathbf{B} \in \mathbb{R}^{N \times p}$ and $\lambda \geq 0$ be given. Then for any $j \in [N]$,*

$$\varphi_\lambda^{\mathbf{B}}(\mathbf{B}_{j,.}) = \text{HSVT}_\lambda(\mathbf{B})_{j,.}^T, \quad (11)$$

where $\mathbf{B}_{j,.} \in \mathbb{R}^{1 \times p}$ represents the j th row of \mathbf{B} , and $\text{HSVT}_\lambda(\mathbf{B})_{j,.} \in \mathbb{R}^{1 \times p}$ represents the j th row of matrix obtained after applying HSVT over \mathbf{B} with threshold λ .

PROOF. By (10), the orthonormality of the right singular vectors and $\mathbf{B}_{j,.}^T = \mathbf{B}^T e_j$ with $e_j \in \mathbb{R}^p$ with j th entry 1 and everything else 0, we have

$$\begin{aligned} \varphi_\lambda^{\mathbf{B}}(\mathbf{B}_{j,.}) &= \sum_{i=1}^{N \wedge p} \mathbb{1}(\sigma_i(\mathbf{B}) \geq \lambda) y_i y_i^T \mathbf{B}_{j,.}^T = \sum_{i=1}^{N \wedge p} \mathbb{1}(\sigma_i(\mathbf{B}) \geq \lambda) y_i y_i^T \mathbf{B}^T e_j \\ &= \sum_{i=1}^{N \wedge p} \mathbb{1}(\sigma_i(\mathbf{B}) \geq \lambda) y_i y_i^T \left(\sum_{i'=1}^{N \wedge p} \sigma_{i'}(\mathbf{B}) x_{i'} y_{i'}^T \right)^T e_j = \sum_{i,i'=1}^{N \wedge p} \sigma_{i'}(\mathbf{B}) \mathbb{1}(\sigma_i(\mathbf{B}) \geq \lambda) y_i y_i^T y_{i'} x_{i'}^T e_j \\ &= \sum_{i,i'=1}^{N \wedge p} \sigma_{i'}(\mathbf{B}) \mathbb{1}(\sigma_i(\mathbf{B}) \geq \lambda) y_i \delta_{ii'} x_{i'}^T e_j = \sum_{i=1}^{N \wedge p} \sigma_i(\mathbf{B}) \mathbb{1}(\sigma_i(\mathbf{B}) \geq \lambda) y_i x_i^T e_j \\ &= \text{HSVT}_\lambda(\mathbf{B})^T e_j = \text{HSVT}_\lambda(\mathbf{B})_{j,.}^T. \end{aligned}$$

□

D CONCENTRATION INEQUALITIES LEMMAS

D.0.1 Classic Results.

THEOREM D.1. Bernstein's Inequality. [4]

Suppose that X_1, \dots, X_n are independent random variables with zero mean, and M is a constant such that $|X_i| \leq M$ with probability one for each i . Let $S := \sum_{i=1}^n X_i$ and $v := \text{Var}(S)$. Then for any $t \geq 0$,

$$\mathbb{P}(|S| \geq t) \leq 2 \exp\left(-\frac{3t^2}{6v + 2Mt}\right).$$

THEOREM D.2. Norm of matrices with sub-gaussian entries. [20]

Let \mathbf{A} be an $m \times n$ random matrix whose entries A_{ij} are independent, mean zero, sub-gaussian random variables. Then, for any $t > 0$, we have

$$\|\mathbf{A}\| \leq CK(\sqrt{m} + \sqrt{n} + t)$$

with probability at least $1 - 2 \exp(-t^2)$. Here, $K = \max_{i,j} \|A_{ij}\|_{\psi_2}$.

LEMMA D.1. Maximum of sequence of random variables. [20]

Let X_1, X_2, \dots, X_n be a sequence of random variables, which are not necessarily independent, and satisfy $\mathbb{E}[X_i^{2p}]^{\frac{1}{2p}} \leq Kp^{\frac{\beta}{2}}$ for some $K, \beta > 0$ and all i . Then, for every $n \geq 2$,

$$\mathbb{E} \max_{i \leq n} |X_i| \leq CK \log^{\frac{\beta}{2}}(n). \quad (12)$$

REMARK D.1. Lemma D.1 implies that if X_1, \dots, X_n are ψ_α random variables with $\|X_i\|_{\psi_\alpha} \leq K_\alpha$ for all $i \in [n]$, then

$$\mathbb{E} \max_{i \leq n} |X_i| \leq CK_\alpha \log^{\frac{1}{\alpha}}(n).$$

D.0.2 High Probability Events for Imputation and Forecasting. Setup. Let \mathbf{X} be an $L \times \bar{P}$ random matrix (with $L \leq \bar{P}$) whose entries X_{ij} are independent sub-gaussian entries where $\mathbb{E}[\mathbf{X}] = \mathbf{M}$ and $\|X_{ij}\|_{\psi_2} \leq \sigma$. Let \mathbf{Y} denote the $L \times \bar{P}$ matrix whose entries Y_{ij} are defined as

$$Y_{ij} = \begin{cases} X_{ij} & \text{w.p. } p, \\ 0 & \text{w.p. } 1 - p, \end{cases}$$

for some $p \in (0, 1]$. Let $\hat{p} = \max \left\{ \frac{1}{L\bar{P}} \sum_{i=1}^L \sum_{j=1}^{\bar{P}} \mathbb{1}_{X_{ij} \text{ observed}}, \frac{1}{L\bar{P}} \right\}$.

High Probability Events. Define events E_1 to E_5 , for some positive absolute constant C as

$$E_1 := \left\{ |\hat{p} - p| \leq p/20 \right\}, \quad (13)$$

$$E_2 := \left\{ \|\mathbf{Y} - p\mathbf{M}\| \leq C\sigma\sqrt{\bar{P}} \right\}, \quad (14)$$

$$E_3 := \left\{ \|\mathbf{Y} - p\mathbf{M}\|_{\infty, 2}^2 \leq C\sigma^2\bar{P} \right\}, \quad (15)$$

$$E_4 := \left\{ \max_{j \in L} \|\varphi_{\lambda_k}^{\mathbf{B}}(Y_{j,\cdot} - p\mathbf{M}_{j,\cdot})\|_2^2 \leq C\sigma^2 k \log(\bar{P}) \right\}, \quad (16)$$

$$E_5 := \left\{ \left(1 - \sqrt{\frac{20 \log(L\bar{P})}{L\bar{P}p}} \right) p \leq \hat{p} \leq \frac{1}{1 - \sqrt{\frac{20 \log(L\bar{P})}{L\bar{P}p}}} p \right\}. \quad (17)$$

Here, $\mathbf{B} \in \mathbb{R}^{L \times \bar{P}}$ is an arbitrary matrix such that $\mathbf{B} = \sum_{i=1}^L \lambda_i(\mathbf{B}) x_i y_i^T$, where $\sigma_i(\mathbf{B})$ are the singular vectors of \mathbf{B} and x_i, y_i are the left and right singular vectors respectively. Recall the definition of $\varphi_{\lambda_k}^{\mathbf{B}}$ in (10).

LEMMA D.2. *For some positive constant c_1*

$$\mathbb{P}(E_1) \geq 1 - 2e^{-c_1 LN p} - (1-p)^{L\bar{P}}, \quad (18)$$

$$\mathbb{P}(E_2) \geq 1 - 2e^{-\bar{P}}, \quad (19)$$

$$\mathbb{P}(E_3) \geq 1 - 2e^{-\bar{P}}, \quad (20)$$

$$\mathbb{P}(E_4) \geq 1 - \frac{2}{L^{10} \bar{P}^{10}}, \quad (21)$$

$$\mathbb{P}(E_5) \geq 1 - \frac{2}{L^{10} \bar{P}^{10}}. \quad (22)$$

PROOF. **Bounding E_1 .** Let $\hat{p}_0 = \frac{1}{LN} \sum_{i=1}^L \sum_{j=1}^N \mathbb{1}_{X_{ij}}$ observed, which implies $\mathbb{E}[\hat{p}_0] = p$. We define the event $E_6 := \{\hat{p}_0 = \hat{p}\}$. Thus, we have that

$$\begin{aligned} \mathbb{P}(E_1^c) &= \mathbb{P}(E_1^c \cap E_6) + \mathbb{P}(E_1^c \cap E_6^c) \\ &= \mathbb{P}(|\hat{p}_0 - p| \geq p/20) + \mathbb{P}(E_1^c \cap E_6^c) \\ &\leq \mathbb{P}(|\hat{p}_0 - p| \geq p/20) + \mathbb{P}(E_6^c) \\ &= \mathbb{P}(|\hat{p}_0 - p| \geq p/20) + (1-p)^{LN}, \end{aligned}$$

where the final equality follows by the independence of observations assumption and the fact that $\hat{p}_0 \neq \hat{p}$ only if we do not have any observations. By Bernstein's Inequality, we have that

$$\mathbb{P}(|\hat{p}_0 - p| \leq p/20) \geq 1 - 2e^{-c_1 LN p}.$$

Bounding E_2 . Since $\mathbb{E}[Y_{ij}] = pM_{ij}$, Theorem D.2 yields

$$\mathbb{P}(E_2) \geq 1 - 2e^{-N}.$$

Bounding E_3 . Observing,

$$\|Y_{j,\cdot} - pM_{j,\cdot}\|_{\infty,2}^2 \leq \|Y_{j,\cdot} - pM_{j,\cdot}\|^2$$

and Theorem D.2 is sufficient to show (20).

Bounding E_4 . Recall $y_i \in \bar{P}$ is the i -th right singular vector of $\mathbf{B} = Y - pM$. Then,

$$\|\varphi_{\lambda_k}^{\mathbf{B}}(Y_{j,\cdot} - pM_{j,\cdot})\|_2^2 = \sum_{i=1}^k \|y_i y_i^T (Y_{j,\cdot} - pM_{j,\cdot})\|_2^2 \leq \sum_{i=1}^k \left(y_i^T (Y_{j,\cdot} - pM_{j,\cdot}) \right)_2^2 = \sum_{i=1}^k Z_i^2,$$

where $Z_i = y_i^T (Y_{j,\cdot} - pM_{j,\cdot})$. By definition of ψ_2 norm of a random variable since y_i is unit norm vector, it follows that

$$\|Z_i\|_{\psi_2} = \|y_i^T (Y_{j,\cdot} - pM_{j,\cdot})\|_{\psi_2} \leq \|(Y_{j,\cdot} - pM_{j,\cdot})\|_{\psi_2}.$$

Since the coordinates of $Y_{j,\cdot} - pM_{j,\cdot}$ are mean-zero and independent, with ψ_2 norm bounded by $\sqrt{C}\sigma$ for some absolute constant $C > 0$, using Lemma H.10 of [2], it follows that

$$\mathbb{P}\left(\sum_{i=1}^k Z_i^2 > t\right) \leq 2k \exp\left(-\frac{t}{kC\sigma^2}\right). \quad (23)$$

Therefore, for choice of $t = C\sigma^2 k \log \bar{P}$ (with large enough constant $C > 0$ and since $L \leq \bar{P}$) and union bound, we have that

$$\mathbb{P}(E_4^c) \leq \frac{2}{L^{10}\bar{P}^{10}}. \quad (24)$$

Bounding E_5 . Recall definition of \hat{p} . Then by the binomial Chernoff bound, for $\varepsilon > 1$,

$$\begin{aligned} \mathbb{P}\left(\hat{p} > \varepsilon p\right) &\leq \exp\left(-\frac{(\varepsilon - 1)^2}{\varepsilon + 1} L \bar{P} p\right), \quad \text{and} \\ \mathbb{P}\left(\hat{p} < \frac{1}{\varepsilon} p\right) &\leq \exp\left(-\frac{(\varepsilon - 1)^2}{2\varepsilon^2} L \bar{P} p\right). \end{aligned}$$

By the union bound,

$$\mathbb{P}\left(\frac{1}{\varepsilon} p \leq \hat{p} \leq p\varepsilon\right) \geq 1 - \mathbb{P}\left(\hat{p} > \varepsilon p\right) - \mathbb{P}\left(\hat{p} < \frac{1}{\varepsilon} p\right).$$

Noticing $\varepsilon + 1 < 2\varepsilon < 2\varepsilon^2$ for all $\varepsilon > 1$, and substituting $\varepsilon = \left(1 - \sqrt{\frac{20 \log(L \bar{P})}{L \bar{P} p}}\right)^{-1}$ completes the proof. \square

COROLLARY D.1. *Let $E := E_1 \cap E_2$. Then,*

$$\mathbb{P}(E^c) \leq C_1 e^{-c_2 \bar{P}}, \quad (25)$$

where C_1 and c_2 are positive constants independent of L and \bar{P} .

COROLLARY D.2. *Let $E := E_2 \cap E_3 \cap E_4 \cap E_5$. Then,*

$$\mathbb{P}(E^c) \leq \frac{C_1}{L^{10}\bar{P}^{10}}, \quad (26)$$

where C_1 is an absolute positive constant, independent of L and \bar{P} .

E HSVT ERROR

LEMMA E.1. *Let $\bar{M}^f = \bar{M}_{(lr)}^f + E_{(lr)}^f$. Recall for $r \in [L - 1]$, let τ_r, μ_r denote the r -th singular value and right singular vector of $\bar{M}_{(lr)}^f$ respectively. Suppose that*

- (1) $\|\bar{Z}^X - \rho \bar{M}^f\| \leq \Delta$ for some $\Delta \geq 0$,
- (2) $\frac{1}{\varepsilon} \rho \leq \hat{\rho} \leq \varepsilon \rho$ for some $\varepsilon \geq 1$,

Let $\bar{\mathbf{M}}_{(lr)}^{f(k)} = \text{HSVT}_{\tau_k}(\bar{\mathbf{M}}_{(lr)})$. Let $\widehat{\mathbf{M}}^{f(k)} = \frac{1}{\rho} \text{HSVT}_{s_k}(\bar{\mathbf{Z}}^X)$, where s_k is the k -th singular value of $\bar{\mathbf{Z}}^X$. Then for any $j \in [L-1]$,

$$\begin{aligned} \left\| \widehat{\mathbf{M}}_{j,\cdot}^{f(k)} - \bar{\mathbf{M}}_{j,\cdot}^f \right\|_2^2 &\leq \frac{8\varepsilon^2}{\rho^4} \left(\frac{\Delta^2 + \|E_{(lr)}^f\|^2}{(\tau_k - \tau_{k+1})^2} \right) \left(\left\| \bar{\mathbf{Z}}_{j,\cdot}^X - \rho \bar{\mathbf{M}}_{j,\cdot}^f \right\|_2^2 + \left\| [\bar{\mathbf{M}}_{(lr)}^{f(k)}]_{j,\cdot} \right\|_2^2 \right) \\ &\quad + \frac{4\varepsilon^2}{\rho^2} \left\| \varphi_{\lambda^*}^Z(\bar{\mathbf{Z}}_{j,\cdot}^X - \rho \bar{\mathbf{M}}_{j,\cdot}^f) \right\|_2^2 + 2(\varepsilon-1)^2 \left\| \bar{\mathbf{M}}_{j,\cdot}^f \right\|_2^2 \\ &\quad + 4 \left\| [E_{(lr)}^f]_{j,\cdot} \right\|_2^2 + 4 \left\| [\bar{\mathbf{M}}_{(lr)}^{f(k)}]_{j,\cdot} \right\|_2^2. \end{aligned} \quad (27)$$

PROOF. For ease of exposition, for the remainder of the proof, let: $\mathbf{A} = \bar{\mathbf{M}}^f$; $\mathbf{Z} = \bar{\mathbf{Z}}^X$; $\widehat{\mathbf{A}} = \widehat{\mathbf{M}}^{f(k)}$; $\mathbf{A}_{(lr)} = \bar{\mathbf{M}}_{(lr)}^f$; $\mathbf{A}_{(lr)}^k = \bar{\mathbf{M}}_{(lr)}^{f(k)}$; $\mathbf{E}_1 = \bar{\mathbf{M}}^f - \bar{\mathbf{M}}_{(lr)}^f$; and $\mathbf{E}_2 = \bar{\mathbf{M}}^f - \bar{\mathbf{M}}_{(lr)}^{f(k)}$.

We will use notation $\lambda^* = s_k$, the k th singular value of $\bar{\mathbf{Z}}^X$ for simplicity. Further, recall that s_r, u_r denote the r -th singular value and right singular vector of $\bar{\mathbf{Z}}^X$ respectively. We prove our Lemma in three steps.

Step 1. Fix a row index $j \in [L-1]$. Observe that

$$\widehat{\mathbf{A}}_{j,\cdot} - \mathbf{A}_{j,\cdot} = \left(\widehat{\mathbf{A}}_{j,\cdot} - \varphi_{\lambda^*}^Z(\mathbf{A}_{j,\cdot}) \right) + \left(\varphi_{\lambda^*}^Z(\mathbf{A}_{j,\cdot}) - \mathbf{A}_{j,\cdot} \right).$$

By definition (see (10)), we have that $\varphi_{\lambda^*}^Z : \mathbb{R}^{\bar{P}} \rightarrow \mathbb{R}^{\bar{P}}$ is the projection operator onto the span of the top k right singular vectors of \mathbf{Z} , namely, $\text{span}\{u_1, \dots, u_k\}$. Therefore,

$$\varphi_{\lambda^*}^Z(\mathbf{A}_{j,\cdot}) - \mathbf{A}_{j,\cdot} \in \text{span}\{u_1, \dots, u_k\}^\perp.$$

By choice, $\text{rank}(\widehat{\mathbf{A}}) = k$; hence, by using Lemma C.1,

$$\widehat{\mathbf{A}}_{j,\cdot} - \varphi_{\lambda^*}^Z(\mathbf{A}_{j,\cdot}) = \frac{1}{\rho} \varphi_{\lambda^*}^Z(\mathbf{Z}_{j,\cdot}) - \varphi_{\lambda^*}^Z(\mathbf{A}_{j,\cdot}) \in \text{span}\{u_1, \dots, u_k\}.$$

Hence, $\langle \widehat{\mathbf{A}}_{j,\cdot} - \varphi_{\lambda^*}^Z(\mathbf{A}_{j,\cdot}), \varphi_{\lambda^*}^Z(\mathbf{A}_{j,\cdot}) - \mathbf{A}_{j,\cdot} \rangle = 0$ and

$$\left\| \widehat{\mathbf{A}}_{j,\cdot} - \mathbf{A}_{j,\cdot} \right\|_2^2 = \left\| \widehat{\mathbf{A}}_{j,\cdot} - \varphi_{\lambda^*}^Z(\mathbf{A}_{j,\cdot}) \right\|_2^2 + \left\| \varphi_{\lambda^*}^Z(\mathbf{A}_{j,\cdot}) - \mathbf{A}_{j,\cdot} \right\|_2^2 \quad (28)$$

by the Pythagorean theorem.

Step 2. We begin by bounding the first term on the right hand side of (28). Again applying Lemma C.1, we can rewrite

$$\begin{aligned} \widehat{\mathbf{A}}_{j,\cdot} - \varphi_{\lambda^*}^Z(\mathbf{A}_{j,\cdot}) &= \frac{1}{\rho} \varphi_{\lambda^*}^Z(\mathbf{Z}_{j,\cdot}) - \varphi_{\lambda^*}^Z(\mathbf{A}_{j,\cdot}) = \varphi_{\lambda^*}^Z \left(\frac{1}{\rho} \mathbf{Z}_{j,\cdot} - \mathbf{A}_{j,\cdot} \right) \\ &= \frac{1}{\rho} \varphi_{\lambda^*}^Z(\mathbf{Z}_{j,\cdot} - \rho \mathbf{A}_{j,\cdot}) + \frac{\rho - \widehat{\rho}}{\widehat{\rho}} \varphi_{\lambda^*}^Z(\mathbf{A}_{j,\cdot}). \end{aligned}$$

Using the Parallelogram Law (or, equivalently, combining Cauchy-Schwartz and AM-GM inequalities), we obtain

$$\begin{aligned}
\|\widehat{\mathbf{A}}_{j,\cdot} - \varphi_{\lambda^*}^Z(\mathbf{A}_{j,\cdot})\|_2^2 &= \left\| \frac{1}{\widehat{\rho}} \varphi_{\lambda^*}^Z(\mathbf{Z}_{j,\cdot} - \rho \mathbf{A}_{j,\cdot}) + \frac{\rho - \widehat{\rho}}{\widehat{\rho}} \varphi_{\lambda^*}^Z(\mathbf{A}_{j,\cdot}) \right\|_2^2 \\
&\leq 2 \left\| \frac{1}{\widehat{\rho}} \varphi_{\lambda^*}^Z(\mathbf{Z}_{j,\cdot} - \rho \mathbf{A}_{j,\cdot}) \right\|_2^2 + 2 \left\| \frac{\rho - \widehat{\rho}}{\widehat{\rho}} \varphi_{\lambda^*}^Z(\mathbf{A}_{j,\cdot}) \right\|_2^2 \\
&\leq \frac{2}{\widehat{\rho}^2} \|\varphi_{\lambda^*}^Z(\mathbf{Z}_{j,\cdot} - \rho \mathbf{A}_{j,\cdot})\|_2^2 + 2 \left(\frac{\rho - \widehat{\rho}}{\widehat{\rho}} \right)^2 \|\mathbf{A}_{j,\cdot}\|_2^2 \\
&\leq \frac{2\epsilon^2}{\rho^2} \|\varphi_{\lambda^*}^Z(\mathbf{Z}_{j,\cdot} - \rho \mathbf{A}_{j,\cdot})\|_2^2 + 2(\epsilon - 1)^2 \|\mathbf{A}_{j,\cdot}\|_2^2.
\end{aligned} \tag{29}$$

because Condition 2 implies $\frac{1}{\widehat{\rho}} \leq \frac{\epsilon}{\rho}$ and $\left(\frac{\rho - \widehat{\rho}}{\widehat{\rho}} \right)^2 \leq (\epsilon - 1)^2$.

Note that the first term of (29) can further be decomposed as,

$$\|\varphi_{\lambda^*}^Z(\mathbf{Z}_{j,\cdot} - \rho \mathbf{A}_{j,\cdot})\|_2^2 \leq 2 \left\| \varphi_{\lambda^*}^Z(\mathbf{Z}_{j,\cdot} - \rho \mathbf{A}_{j,\cdot}) - \varphi^{A_{(lr)}^k}(\mathbf{Z}_{j,\cdot} - \rho \mathbf{A}_{j,\cdot}) \right\|_2^2 + 2 \left\| \varphi^{A_{(lr)}^k}(\mathbf{Z}_{j,\cdot} - \rho \mathbf{A}_{j,\cdot}) \right\|_2^2. \tag{30}$$

We now bound the first term on the right hand side of (30) separately. First, we apply the Davis-Kahan sin Θ Theorem (see [6, 22]) to arrive at the following inequality:

$$\|\mathcal{P}_{u_1, \dots, u_k} - \mathcal{P}_{\mu_1, \dots, \mu_k}\|_2 \leq \frac{\|\mathbf{Z} - \rho \mathbf{A}_{(lr)}\|}{\rho \tau_k - \rho \tau_{k+1}} \tag{31}$$

$$\leq \frac{\|\mathbf{Z} - \rho \mathbf{A}\|}{\rho \tau_k - \rho \tau_{k+1}} + \frac{\|\rho \mathbf{A} - \rho \mathbf{A}_{(lr)}\|}{\rho \tau_k - \rho \tau_{k+1}} \tag{32}$$

$$\leq \frac{\Delta}{\rho(\tau_k - \tau_{k+1})} + \frac{\|E_1\|}{\tau_k - \tau_{k+1}} \tag{33}$$

where $\mathcal{P}_{u_1, \dots, u_k}$ and $\mathcal{P}_{\mu_1, \dots, \mu_k}$ denote the projection operators onto the span of the top k right singular vectors of \mathbf{Z} and $\mathbf{A}_{(lr)}$, respectively. Note, we utilized Condition 1 to bound $\|\mathbf{Z} - \rho \mathbf{A}\|_2 \leq \Delta$.

Then it follows that

$$\begin{aligned}
\left\| \varphi_{\lambda^*}^Z(\mathbf{Z}_{j,\cdot} - \rho \mathbf{A}_{j,\cdot}) - \varphi^{A_{(lr)}^k}(\mathbf{Z}_{j,\cdot} - \rho \mathbf{A}_{j,\cdot}) \right\|_2 &\leq \|\mathcal{P}_{u_1, \dots, u_k} - \mathcal{P}_{\mu_1, \dots, \mu_k}\|_2 \|\mathbf{Z}_{j,\cdot} - \rho \mathbf{A}_{j,\cdot}\|_2 \\
&\leq \left(\frac{\Delta}{\rho(\tau_k - \tau_{k+1})} + \frac{\|E_1\|}{\tau_k - \tau_{k+1}} \right) \|\mathbf{Z}_{j,\cdot} - \rho \mathbf{A}_{j,\cdot}\|_2.
\end{aligned}$$

Combining the inequalities together, we have

$$\begin{aligned}
\|\widehat{\mathbf{A}}_{j,\cdot} - \varphi_{\lambda^*}^Z(\mathbf{A}_{j,\cdot})\|_2^2 &\leq \frac{8\epsilon^2}{\rho^4} \left(\frac{\Delta^2}{(\tau_k - \tau_{k+1})^2} + \frac{\|E_1\|^2}{(\tau_k - \tau_{k+1})^2} \right) \|\mathbf{Z}_{j,\cdot} - \rho \mathbf{A}_{j,\cdot}\|_2^2 \\
&\quad + \frac{4\epsilon^2}{\rho^2} \left\| \varphi^{A_{(lr)}^k}(\mathbf{Z}_{j,\cdot} - \rho \mathbf{A}_{j,\cdot}) \right\|_2^2 + 2(\epsilon - 1)^2 \|\mathbf{A}_{j,\cdot}\|_2^2.
\end{aligned} \tag{34}$$

Step 3. We now bound the second term of (28). Recalling $\mathbf{A} = \mathbf{A}_{(lr)}^k + \mathbf{E}_2$ and using (31)

$$\begin{aligned}
\|\varphi_{\lambda^*}^Z(\mathbf{A}_{j,\cdot}) - \mathbf{A}_{j,\cdot}\|_2^2 &= \|\varphi_{\lambda^*}^Z([A_{(lr)}^k]_{j,\cdot} + [E_2]_{j,\cdot}) - [A_{(lr)}^k]_{j,\cdot} - [E_2]_{j,\cdot}\|_2^2 \\
&\leq 2 \|\varphi_{\lambda^*}^Z([A_{(lr)}^k]_{j,\cdot}) - [A_{(lr)}^k]_{j,\cdot}\|_2^2 + 2 \|\varphi_{\lambda^*}^Z([E_2]_{j,\cdot}) - [E_2]_{j,\cdot}\|_2^2 \\
&= 2 \|\varphi_{\lambda^*}^Z([A_{(lr)}^k]_{j,\cdot}) - \varphi^{A^k}([A_{(lr)}^k]_{j,\cdot})\|_2^2 + 2 \|\varphi_{\lambda^*}^Z([E_2]_{j,\cdot}) - [E_2]_{j,\cdot}\|_2^2 \\
&\leq 2 \|\mathcal{P}_{u_1, \dots, u_{k_{(lr)}}} - \mathcal{P}_{\mu_1, \dots, \mu_k}\|_2^2 \|[A_{(lr)}^k]_{j,\cdot}\|_2^2 + 2 \|[E_2]_{j,\cdot}\|_2^2 \\
&\leq 4 \left(\frac{\Delta^2}{\rho^2(\tau_k - \tau_{k+1})^2} + \frac{\|E_1\|^2}{(\tau_k - \tau_{k+1})^2} \right) \|[A_{(lr)}^k]_{j,\cdot}\|_2^2 + 2 \|[E_2]_{j,\cdot}\|_2^2.
\end{aligned} \tag{35}$$

Inserting (34) and (35) back to (28), and collecting terms completes the proof. \square

COROLLARY E.1. *Let the conditions of Lemma E.1 hold. Then for any $j \in [L-1]$,*

$$\begin{aligned} \left\| \widehat{\mathbf{M}}_{j,\cdot}^{f(k)} - \bar{\mathbf{M}}_{j,\cdot}^f \right\|_2^2 &\leq \frac{8\varepsilon^2}{\rho^4} \left(\frac{\Delta^2 + L\bar{P}(R\epsilon_{\max}\Gamma_1)^2}{(\tau_k - \tau_{k+1})^2} \right) \left(\left\| \bar{\mathbf{Z}}_{j,\cdot}^X - \rho \bar{\mathbf{M}}_{j,\cdot}^f \right\|_2^2 + \left\| [\bar{\mathbf{M}}_{(lr)}^{f(k)}]_{j,\cdot} \right\|_2^2 \right) \\ &\quad + \frac{4\varepsilon^2}{\rho^2} \left\| \varphi \bar{\mathbf{M}}_{(lr)}^{f(k)} (\bar{\mathbf{Z}}_{j,\cdot}^X - \rho \bar{\mathbf{M}}_{j,\cdot}^f) \right\|_2^2 + 2(\varepsilon - 1)^2 \left\| \bar{\mathbf{M}}_{j,\cdot}^f \right\|_2^2 \\ &\quad + 4\bar{P}(R\epsilon_{\max}\Gamma_1)^2 + 4 \left\| [\bar{\mathbf{M}}_{(lr)}^f - \bar{\mathbf{M}}_{(lr)}^{f(k)}]_{j,\cdot} \right\|_2^2. \end{aligned} \quad (36)$$

PROOF. Immediate from Lemma E.1 and Proposition 2.6. \square

PROPOSITION E.1. *Assume Properties 2.1, 2.3, 2.4 and 2.2 hold. Then,*

$$\begin{aligned} \mathbb{E} \left\| \bar{\mathbf{M}}^f - \widehat{\mathbf{M}}^{f(k)} \right\|_{\infty,2}^2 &\leq \frac{C^*(\gamma^2, R^2, \Gamma_1^2, \Gamma_2^2)}{\rho^4} \left(\frac{1}{(\tau_k - \tau_{k+1})^2} + \frac{k}{\bar{P}^2} + \frac{L((\epsilon_{\max})^2 + (\epsilon_{\max})^4)}{(\tau_k - \tau_{k+1})^2} \right) \log(\bar{P})\bar{P}^2 \\ &\quad + 4 \max_{j \in [L-1]} \left\| [\bar{\mathbf{M}}_{(lr)}^f - \bar{\mathbf{M}}_{(lr)}^{f(k)}]_{j,\cdot} \right\|_2^2, \end{aligned} \quad (37)$$

where $C^*(\gamma^2, R^2, \Gamma_1^2, \Gamma_2^2)$ is a term that depends only on $\gamma^2, R^2, \Gamma_1^2, \Gamma_2^2$.

PROOF. Notation. For ease of exposition, for the remainder of the proof, let: $\mathbf{A} = \bar{\mathbf{M}}^f$; $\mathbf{Z} = \bar{\mathbf{Z}}^X$; $\widehat{\mathbf{A}} = \widehat{\mathbf{M}}^{f(k)}$; $\mathbf{A}_{(lr)} = \bar{\mathbf{M}}_{(lr)}^f$; $\mathbf{A}_{(lr)}^k = \bar{\mathbf{M}}_{(lr)}^{f(k)}$; and $\mathbf{E} = \bar{\mathbf{M}}_{(lr)}^f - \bar{\mathbf{M}}_{(lr)}^{f(k)}$.

High Probability Conditioning Event. Let $E := E_2 \cap E_3 \cap E_4 \cap E_5$ where E_2 to E_5 are defined in (14) to (17) respectively. Then,

$$\begin{aligned} \mathbb{E}[\|\widehat{\mathbf{A}} - \mathbf{A}\|_{\infty,2}^2] &= \mathbb{E} \max_{j \in [L-1]} \left\| \widehat{\mathbf{A}}_{j,\cdot} - \mathbf{A}_{j,\cdot} \right\|_2^2 \\ &= \mathbb{E} \left[\max_{j \in [L-1]} \left\| \widehat{\mathbf{A}}_{j,\cdot} - \mathbf{A}_{j,\cdot} \right\|_2^2 \cdot \mathbb{1}(E) \right] + \mathbb{E} \left[\max_{j \in [L-1]} \left\| \widehat{\mathbf{A}}_{j,\cdot} - \mathbf{A}_{j,\cdot} \right\|_2^2 \cdot \mathbb{1}(E^c) \right]. \end{aligned} \quad (38)$$

Upper bound on the first term in (38). First note $\varepsilon^2 \leq 10$ since $\rho \geq \frac{64 \log(\bar{P}L)}{\bar{P}L}$; and that

$$\left\| [\mathbf{A}_{(lr)}^k]_{j,\cdot} \right\|_2^2 \leq \left\| \mathbf{A}_{j,\cdot}^k \right\|_2^2 \stackrel{(a)}{\leq} (R\Gamma_1(\Gamma_2 + \epsilon_{\max}))^2 \bar{P}$$

where (a) follows by Lemma B.1 and Proposition 2.6. Then conditioned on event E , and by Corollary E.1,

$$\begin{aligned} \max_{j \in [L-1]} \left\| \widehat{\mathbf{A}}_{j,\cdot} - \mathbf{A}_{j,\cdot} \right\|_2^2 &\leq \frac{C}{\rho^4} \left(\frac{\gamma^2 \bar{P} + L\bar{P}(R\epsilon_{\max}\Gamma_1)^2}{(\tau_k - \tau_{k+1})^2} \right) \left(\gamma^2 \bar{P} + (R\Gamma_1(\Gamma_2 + \epsilon_{\max}))^2 \bar{P} \right) \\ &\quad + \frac{C}{\rho^2} \left(\gamma^2 k \log(\bar{P}) \right) + 2\bar{P}(R\epsilon_{\max}\Gamma_1)^2 + 4 \max_{j \in [L-1]} \left\| \mathbf{E}_{j,\cdot} \right\|_2^2. \end{aligned} \quad (39)$$

Simplifying (39) by collecting terms, we have

$$\begin{aligned} \max_{j \in [L-1]} \left\| \widehat{\mathbf{A}}_{j,\cdot} - \mathbf{A}_{j,\cdot} \right\|_2^2 &\leq \frac{C^*(\gamma^2, R^2, \Gamma_1^2, \Gamma_2^2)}{\rho^4} \left(\frac{1}{(\tau_k - \tau_{k+1})^2} + \frac{k}{\bar{P}^2} + \frac{L((\epsilon_{\max})^2 + (\epsilon_{\max})^4)}{(\tau_k - \tau_{k+1})^2} \right) \log(\bar{P})\bar{P}^2 \\ &\quad + 4 \max_{j \in [L-1]} \left\| \mathbf{E}_{j,\cdot} \right\|_2^2. \end{aligned} \quad (40)$$

where $C^*(\gamma^2, R^2, \Gamma_1^2, \Gamma_2^2)$ is a term that depends only on $\gamma^2, R^2, \Gamma_1^2, \Gamma_2^2$.

Since $\mathbb{P}(E) \leq 1$, we have

$$\begin{aligned} \mathbb{E} \left[\max_{j \in [L-1]} \|\widehat{\mathbf{A}}_{j,\cdot} - \mathbf{A}_{j,\cdot}\|_2^2 \cdot \mathbb{1}(E) \right] &\leq \frac{C^*(\gamma^2, R^2, \Gamma_1^2, \Gamma_2^2)}{\rho^4} \left(\frac{1}{(\tau_k - \tau_{k+1})^2} + \frac{k}{\bar{P}^2} + \frac{L((\epsilon_{\max})^2 + (\epsilon_{\max})^4)}{(\tau_k - \tau_{k+1})^2} \right) \log(\bar{P}) \bar{P}^2 \\ &\quad + 4 \max_{j \in [L-1]} \|E_{j,\cdot}\|_2^2 \end{aligned} \quad (41)$$

Upper bound on the second term in (38). To begin with, we note that for any $j \in [L-1]$,

$$\|\widehat{\mathbf{A}}_{j,\cdot} - \mathbf{A}_{j,\cdot}\|_2 \leq \|\widehat{\mathbf{A}}_{j,\cdot}\|_2 + \|\mathbf{A}_{j,\cdot}\|_2$$

by triangle inequality. By the model assumption, the covariates are bounded (Property 2.1) and $\|\mathbf{A}_{j,\cdot}\|_2 \leq (R\Gamma_1\Gamma_2)\sqrt{\bar{P}}$ for all $j \in [L-1]$. For the remainder of the proof, for ease of notation, let $\Gamma := (R\Gamma_1\Gamma_2)$. By definition, for any $j \in [L-1]$,

$$\widehat{\mathbf{A}}_{j,\cdot} = \frac{1}{\bar{\rho}} \text{HSVT}_\lambda(\mathbf{Z})_{\cdot,j}$$

for a given threshold $\lambda = s_k$, the k th singular value of \mathbf{Z} . Therefore,

$$\|\widehat{\mathbf{A}}_{j,\cdot}\|_2 = \frac{1}{\bar{\rho}} \|\text{HSVT}_\lambda(\mathbf{Z})_{\cdot,j}\|_2 \stackrel{(a)}{\leq} \bar{P}L \|\text{HSVT}_\lambda(\mathbf{Z})_{\cdot,j}\|_2 \leq \bar{P}L \|\mathbf{Z}_{\cdot,j}\|_2.$$

Here, (a) follows from $\bar{\rho} \geq \frac{1}{\bar{P}L}$.

$$\begin{aligned} \max_{j \in [L-1]} \|\widehat{\mathbf{A}}_{j,\cdot} - \mathbf{A}_{j,\cdot}\|_2 &\leq \max_{j \in [L-1]} \|\widehat{\mathbf{A}}_{j,\cdot}\|_2 + \max_{j \in [p]} \|\mathbf{A}_{j,\cdot}\|_2 \\ &\leq \bar{P}L \max_{j \in [L-1]} \|\mathbf{Z}_{\cdot,j}\|_2 + \Gamma \sqrt{\bar{P}} \\ &\leq (\bar{P}^{\frac{3}{2}}L + \sqrt{\bar{P}})\Gamma + \bar{P}^{\frac{3}{2}}L \max_{ij} |\eta_{ij}| \\ &\leq 2\bar{P}^{\frac{3}{2}}L \left(\Gamma + \max_{ij} |\eta_{ij}| \right) \end{aligned} \quad (42)$$

because $\max_{j \in [p]} \|\mathbf{Z}_{\cdot,j}\|_2 \leq \sqrt{\bar{P}} \max_{i,j} |Z_{ij}| \leq \sqrt{\bar{P}} \max_{i,j} |A_{ij} + \eta_{ij}| \leq \sqrt{\bar{P}}(\Gamma + \max_{i,j} |\eta_{ij}|)$. Now we apply Cauchy-Schwarz inequality on $\mathbb{E} \left[\max_{j \in [L-1]} \|\widehat{\mathbf{A}}_{j,\cdot} - \mathbf{A}_{j,\cdot}\|_2^2 \cdot \mathbb{1}(E^c) \right]$ to obtain

$$\begin{aligned} \mathbb{E} \left[\max_{j \in [L-1]} \|\widehat{\mathbf{A}}_{j,\cdot} - \mathbf{A}_{j,\cdot}\|_2^2 \cdot \mathbb{1}(E^c) \right] &\leq \mathbb{E} \left[\max_{j \in [L-1]} \|\widehat{\mathbf{A}}_{j,\cdot} - \mathbf{A}_{j,\cdot}\|_2^4 \right]^{\frac{1}{2}} \cdot \mathbb{E} \left[\mathbb{1}(E^c) \right]^{\frac{1}{2}} \\ &= \mathbb{E} \left[\max_{j \in [L-1]} \|\widehat{\mathbf{A}}_{j,\cdot} - \mathbf{A}_{j,\cdot}\|_2^4 \right]^{\frac{1}{2}} \cdot \mathbb{P}(E^c)^{\frac{1}{2}} \\ &\stackrel{(a)}{\leq} 4\bar{P}^3 L^2 \mathbb{E} \left[\left(\Gamma + \max_{ij} |\eta_{ij}| \right)^4 \right]^{\frac{1}{2}} \cdot \mathbb{P}(E^c)^{\frac{1}{2}} \\ &\stackrel{(b)}{\leq} 8\sqrt{2}\bar{P}^3 L^2 \left(\Gamma^4 + \mathbb{E} \left[\max_{ij} |\eta_{ij}|^4 \right] \right)^{\frac{1}{2}} \cdot \mathbb{P}(E^c)^{\frac{1}{2}} \\ &\stackrel{(c)}{\leq} 8\sqrt{2}\bar{P}^3 L^2 \left(\Gamma^2 + \mathbb{E} \left[\max_{ij} |\eta_{ij}|^4 \right]^{\frac{1}{2}} \right) \cdot \mathbb{P}(E^c)^{\frac{1}{2}}. \end{aligned} \quad (43)$$

Here, (a) follows from (42); and (b) follows from Jensen's inequality:

$$\begin{aligned} \mathbb{E} \left[\left(\Gamma + \max_{ij} |\eta_{ij}| \right)^4 \right] &= \mathbb{E} \left[\left(\frac{1}{2} (2\Gamma + 2 \max_{ij} |\eta_{ij}|) \right)^4 \right] \leq \mathbb{E} \left[\frac{1}{2} \left((2\Gamma)^4 + (2 \max_{ij} |\eta_{ij}|)^4 \right) \right] \\ &= 8\mathbb{E} \left[\Gamma^4 + \max_{ij} |\eta_{ij}|^4 \right] = 8 \left(\Gamma^4 + \mathbb{E} \left[\max_{ij} |\eta_{ij}|^4 \right] \right); \end{aligned}$$

and (c) follows from the trivial inequality: $\sqrt{A+B} \leq \sqrt{A} + \sqrt{B}$ for any $A, B \geq 0$.

Now it remains to find an upper bound for $\mathbb{E}[\max_{ij} |\eta_{ij}|^4]$. Note that for $\theta \geq 1$, η_{ij} being a ψ_2 -random variable implies that $|\eta_{ij}|^\theta$ is a $\psi_{2/\theta}$ -random variable. With the choice of $\theta = 4$, we have that

$$\mathbb{E} \max_{ij} |\eta_{ij}|^4 \leq C' \gamma^4 \log^2(\bar{P}L) \quad (44)$$

for some $C' > 0$ by Lemma D.1 (also see Remark D.1). Inserting (44) to (43) yields

$$\begin{aligned} \mathbb{E} \left[\max_{j \in [L-1]} \|\widehat{\mathbf{A}}_{j,\cdot} - \mathbf{A}_{j,\cdot}\|_2^2 \cdot \mathbb{1}(E^c) \right] &\leq 8\sqrt{2}\bar{P}^3L^2 \left(\Gamma^2 + C'^{1/2}\gamma^2 \log(\bar{P}L) \right) \cdot \mathbb{P}(E^c)^{\frac{1}{2}} \\ &\stackrel{(a)}{\leq} 32 \left(\Gamma^2 + C'^{1/2}\gamma^2 \log(\bar{P}L) \right) \frac{1}{\bar{P}^2L^3}, \end{aligned} \quad (45)$$

where (a) follows from recalling that $\mathbb{P}(E^c) \leq \frac{8}{\bar{P}^{10}L^{10}}$.

Concluding the Proof. Thus, combining (41) and (45) in (38) and noticing that term in (45) is smaller order term than that in (41), by redefining $C^*(\gamma^2, R^2, \Gamma_1^2, \Gamma_2^2)$, appropriately we obtain the desired bound:

$$\begin{aligned} \mathbb{E} \left[\|\widehat{\mathbf{A}}_{j,\cdot} - \mathbf{A}_{j,\cdot}\|_{\infty,2}^2 \right] &\leq \frac{C^*(\gamma^2, R^2, \Gamma_1^2, \Gamma_2^2)}{\rho^4} \left(\frac{1}{(\tau_k - \tau_{k+1})^2} + \frac{k}{\bar{P}^2} + \frac{L((\epsilon_{\max})^2 + (\epsilon_{\max})^4)}{(\tau_k - \tau_{k+1})^2} \right) \log(\bar{P})\bar{P}^2 \\ &\quad + 4 \max_{j \in [L-1]} \|\mathbf{E}_{j,\cdot}\|_2^2 \end{aligned} \quad (46)$$

□

F PROOFS - IMPUTATION ANALYSIS

F.1 Proof of Theorem 4.1

PROOF. Observe that for any matrix, $\mathbf{A} \in \mathbb{R}^{m \times n}$,

$$\frac{1}{n} \|\mathbf{A}\|_{\infty,2}^2 \geq \frac{1}{mn} \|\mathbf{A}\|_F^2.$$

Then using Property 4.1 and Proposition E.1, and simplifying terms gives the desired result. □

G PROOFS - FORECASTING ANALYSIS

G.1 Forecasting - Helper Lemmas

PROPOSITION G.1. *Let Properties 2.1 and 2.2 hold. Then there exists $\beta^* \in \mathbb{R}^{L-1}$, with $\|\beta^*\|_1 \leq CRG_{\max}$, such that*

$$\|(\bar{\mathbf{M}}^f)^T \beta^* - \mathbf{M}_L^f\|_\infty \leq C(R)^2(G_{\max} + 1)\epsilon_{\max}\Gamma_1. \quad (47)$$

Here C is an absolute constant.

PROOF. To reduce notational complexity, we suppress the superscript f for the remainder of the proof.

Let \mathbf{H} and $\mathbf{H}_{(lr)}$ be defined as in Proposition 2.6. Since $\text{rank}(\mathbf{H}_{(lr)}) \leq RG_{\max}$, it must be the case that within the last RG_{\max} rows, there exists at least one row (which we denote as r^*) that can be written as a linear combination of at most RG_{\max} rows above it (which we denote as $r_1, \dots, r_{RG_{\max}}$). Solely for the purposes of the remainder of the proof (and without any loss of generality), we redefine $\mathbf{M}, \mathbf{H}, \mathbf{H}_{(lr)}$ assuming access to data $t \in [-T : 2T]$ (instead of $[1 : T]$).

Specifically there exists $\theta_l \in \mathbb{R}$ for $l \in [RG_{\max}]$, such that for all $t \in [L : T]$ ⁹

$$[\mathbf{H}_{(lr)}]_{(r^*,t)} = \sum_{l=1}^{RG_{\max}} \theta_l [\mathbf{H}_{(lr)}]_{(r_l,t)}. \quad (48)$$

⁹Here is where we use the fact that we redefined $\mathbf{M}, \mathbf{H}, \mathbf{H}_{(lr)}$ with respect to $t \in [-T : 2T]$. Otherwise, we could only claim the equality in (48) for $t \in [L : T - RG_{\max}]$

Hence for all $t \in [0 : T]$,

$$\begin{aligned}
\left| [\mathbf{H}]_{(r^*, t)} - \sum_{l=1}^{RG_{\max}} \theta_l [\mathbf{H}]_{(r_l, t)} \right| &= \left| [\mathbf{H}]_{(r^*, t)} \pm [\mathbf{H}_{(lr)}]_{(r^*, t)} - \sum_{l=1}^{RG_{\max}} \theta_l [\mathbf{H}]_{(r_l, t)} \pm \sum_{l=1}^{RG_{\max}} \theta_l [\mathbf{H}_{(lr)}]_{(r_l, t)} \right| \\
&\leq \left| [\mathbf{H}]_{(r^*, t)} - [\mathbf{H}_{(lr)}]_{(r^*, t)} \right| + \left| \sum_{l=1}^{RG_{\max}} \theta_l [\mathbf{H}]_{(r_l, t)} - \sum_{l=1}^{RG_{\max}} \theta_l [\mathbf{H}_{(lr)}]_{(r_l, t)} \right| \\
&\quad + \left| [\mathbf{H}_{(lr)}]_{(r^*, t)} - \sum_{l=1}^{RG_{\max}} \theta_l [\mathbf{H}_{(lr)}]_{(r_l, t)} \right| \\
&= \left| [\mathbf{H}]_{(r^*, t)} - [\mathbf{H}_{(lr)}]_{(r^*, t)} \right| + \left| \sum_{l=1}^{RG_{\max}} \theta_l [\mathbf{H}]_{(r_l, t)} - \sum_{l=1}^{RG_{\max}} \theta_l [\mathbf{H}_{(lr)}]_{(r_l, t)} \right| \\
&\stackrel{(a)}{\leq} C \left(R\epsilon_{\max} \Gamma_1 + (RG_{\max}) R\epsilon_{\max} \Gamma_1 \right) \\
&\leq C(R)^2 (G_{\max} + 1) \epsilon_{\max} \Gamma_1
\end{aligned}$$

where (a) follows from Proposition 2.6 and C is an absolute constant.

Observing that every entry of \mathbf{M}_L^f appears in $[\mathbf{H}]_{(r^*, \cdot)}$ and letting $\beta^* := (\theta_1, \dots, \theta_{RG_{\max}})$ completes the proof by redefining constants appropriately. \square

PROPOSITION G.2. *Assume Properties 2.1, 2.3, 2.4 and 2.2 hold. Then for some absolute constants, $C_1 \geq 0$,*

$$\text{MSE}(\mathbf{M}^f, \widehat{\mathbf{M}}^{f(\text{Forecast})}) \leq C_1 \left((R)^2 (G_{\max} + 1) \epsilon_{\max} \Gamma_1 \right)^2 + C_1 \left(RG_{\max} \right)^2 \frac{\mathbb{E} \left\| \bar{\mathbf{M}}^f - \widehat{\mathbf{M}}^{f,k} \right\|_{\infty, 2}^2}{\bar{P}} + \tilde{K}^2 \frac{k}{\bar{P}},$$

where $\widehat{\mathbf{M}}^{f,k}$ is the estimation obtained in the first step of the forecasting algorithm in Section 3.1 using threshold $k \geq 1$ for number of singular values, \tilde{K} is function of $\gamma^2, R, \Gamma_1, \Gamma_2, \rho^{-1}$.

PROOF. Let $\mathbf{Q} := \rho(\bar{\mathbf{M}}^f)^T$ and $\widehat{\mathbf{Q}} := \rho(\widehat{\mathbf{M}}^{f,k})^T$. Define $\eta_L \in \mathbb{R}^{\bar{P}}$, where $\eta_L := Z_L^X - \rho \mathbf{M}_L^f$. For each entry in Z_L^X , it is equal to the noisy version underlying time series with probability ρ , and otherwise 0; and the noisy version has additive noise added to the corresponding entry in the component of \mathbf{M}_L^f . Therefore, $\mathbb{E}[\eta_L] = \mathbf{0}$ and using Property 2.4 as well as Lemma G.2 in [2], it follows that the coordinates of η_L are independent mean-zero sub-gaussian random variables such that $\|\eta_L(s)\|_{\psi_2} \leq C'(\gamma^2 + R\Gamma_1\Gamma_2)$ for $s \in \mathbb{R}^{\bar{P}}$, where $C' > 0$ is an absolute constant. Define $K(\gamma^2, R, \Gamma_1, \Gamma_2) := C'(\gamma^2 + R\Gamma_1\Gamma_2)$.

Let β^* below be defined as in Proposition G.1. Then note that by the definition of $\hat{\beta}$ in the algorithm,

$$\begin{aligned}
\|Z_L^X - \widehat{\mathbf{Q}}\hat{\beta}\|_2^2 &\leq \|Z_L^X - \widehat{\mathbf{Q}}\beta^*\|_2^2 \\
&= \|\rho \mathbf{M}_L^f - \widehat{\mathbf{Q}}\beta^*\|_2^2 + \|\eta_L\|_2^2 + 2\eta_L^T(\rho \mathbf{M}_L^f - \widehat{\mathbf{Q}}\beta^*). \tag{49}
\end{aligned}$$

Moreover,

$$\|Z_L^X - \widehat{\mathbf{Q}}\hat{\beta}\|_2^2 = \|\mathbf{M}_L^f - \widehat{\mathbf{Q}}\hat{\beta}\|_2^2 + \|\eta_L\|_2^2 - 2\eta_L^T(\widehat{\mathbf{Q}}\hat{\beta} - \rho \mathbf{M}_L^f). \tag{50}$$

Combining (49) and (50) and taking expectations, we have

$$\mathbb{E} \|\rho \mathbf{M}_L^f - \widehat{\mathbf{Q}}\hat{\beta}\|_2^2 \leq \mathbb{E} \|\rho \mathbf{M}_L^f - \widehat{\mathbf{Q}}\beta^*\|_2^2 + 2\mathbb{E}[\eta_L^T \widehat{\mathbf{Q}}(\hat{\beta} - \beta^*)]. \tag{51}$$

Let us bound the final term on the right hand side of (51). Under our independence assumptions, observe that

$$\mathbb{E}[\eta_L^T \widehat{Q}] \beta^* = \mathbb{E}[\eta_L^T] \mathbb{E}[\widehat{Q}] \beta^* = 0. \quad (52)$$

Recall $\widehat{\beta} = \widehat{Q}^\dagger Z_L^X = \rho \widehat{Q}^\dagger M_L^f + \widehat{Q}^\dagger \eta_L$. Using the cyclic and linearity properties of the trace operator (coupled with similar independence arguments), we further have

$$\begin{aligned} \mathbb{E}[\eta_L^T \widehat{Q} \widehat{\beta}] &= \mathbb{E}[\rho \eta_L^T \widehat{Q} \widehat{Q}^\dagger] M_L^f + \mathbb{E}[\eta_L^T \widehat{Q} \widehat{Q}^\dagger \eta_L] \\ &= \mathbb{E}[\text{Tr}(\eta_L^T \widehat{Q} \widehat{Q}^\dagger \eta_L)] \\ &= \mathbb{E}[\text{Tr}(\widehat{Q} \widehat{Q}^\dagger \eta_L \eta_L^T)] \\ &= \text{Tr}(\mathbb{E}[\widehat{Q} \widehat{Q}^\dagger] \cdot \mathbb{E}[\eta_L \eta_L^T]) \\ &\stackrel{(a)}{\leq} C_\gamma K(\rho, \gamma)^2 \mathbb{E}[\text{Tr}(\widehat{Q} \widehat{Q}^\dagger)], \end{aligned} \quad (53)$$

where (a) follows from Property 2.4. Here C_γ is an absolute constant that may depend on γ as well as ρ .

Let $\widehat{Q} = USV^T$ be the singular value decomposition of \widehat{Q} . Then

$$\begin{aligned} \widehat{Q} \widehat{Q}^\dagger &= USV^T V S^\dagger U^T \\ &= U \tilde{I} U^T. \end{aligned} \quad (54)$$

Here, \tilde{I} is a block diagonal matrix where its nonzero entries on the diagonal take the value 1. Plugging in (54) into (53), and using the fact that the trace of a square matrix is equal to the sum of its eigenvalues,

$$\mathbb{E}[\text{Tr}(\widehat{Q} \widehat{Q}^\dagger)] = \mathbb{E}[\text{rank}(\widehat{Q})] = k. \quad (55)$$

We now turn our attention to the first term on the right hand side of (51). We obtain

$$\begin{aligned} \|\rho M_L^f - \widehat{Q} \beta^*\|_2^2 &= \|\rho M_L^f - (Q - Q + \widehat{Q}) \beta^*\|_2^2 \\ &\leq 2\|\rho M_L^f - Q \beta^*\|_2^2 + 2\|(Q - \widehat{Q}) \beta^*\|_2^2 \\ &\stackrel{(a)}{\leq} 2\rho^2 \left((R)^2 (G_{\max} + 1) \epsilon_{\max} \Gamma_1 \right)^2 \bar{P} + 2\|(Q - \widehat{Q}) \beta^*\|_2^2, \end{aligned}$$

where (a) follows from Proposition G.1.

We also have,

$$\mathbb{E}\|(Q - \widehat{Q}) \beta^*\|_2^2 = \rho^2 \mathbb{E}\left\| \left(\bar{M}^f - \widehat{M}^{f,k} \right)^T \beta^* \right\|_2^2 \quad (56)$$

$$\leq \rho^2 \|\beta^*\|_1^2 \mathbb{E}\| \bar{M}^f - \widehat{M}^{f,k} \|_{\infty,2}^2 \quad (57)$$

$$\stackrel{(b)}{\leq} \rho^2 \left(CRG_{\max} \right)^2 \mathbb{E}\| \bar{M}^f - \widehat{M}^{f,k} \|_{\infty,2}^2, \quad (58)$$

where (b) follows from Proposition G.1.

Collecting all the terms together, dividing by $\rho^2 \times \bar{P}$, using $\tilde{K}(\gamma^2, R, \Gamma_1, \Gamma_2, \rho^{-1}) = K(\gamma^2, R, \Gamma_1, \Gamma_2)/\rho$ and redefining the constants, we obtain our desired result. \square

THEOREM G.1. Assume Properties 2.1, 2.3, 2.4 and 2.2 hold. Further, let (i) $\bar{P} \geq L$. Then,

$$\begin{aligned} & \text{MSE}(\mathcal{M}^f, \tilde{\mathcal{M}}^{f(\text{Forecast})}) \\ & \leq \frac{C^*(\gamma^2, R^2, \Gamma_1^2, \Gamma_2^2, (G_{\max})^2)}{\rho^4} \left(\frac{\bar{P} + \bar{P}L((\epsilon_{\max})^2 + (\epsilon_{\max})^4)}{(\tau_k - \tau_{k+1})^2} + \frac{k}{\bar{P}} \tilde{K}(\gamma^2, R, \Gamma_1, \Gamma_2, \rho^{-1}) + (\epsilon_{\max})^2 \right) \log(\bar{P}) \\ & \quad + \frac{C(RG_{\max})^2}{\bar{P}} \left\| \tilde{\mathcal{M}}_{(lr)}^f - \tilde{\mathcal{M}}_{(lr)}^{f(k)} \right\|_{\infty, 2}^2, \end{aligned}$$

where $C^*(\gamma^2, R^2, \Gamma_1^2, \Gamma_2^2)$ is a term that depends only on $\gamma^2, R^2, \Gamma_1^2, \Gamma_2^2$ and $C \geq 0$ is an absolute constant. Here, $\tilde{K}(\gamma^2, R, \Gamma_1, \Gamma_2, \rho^{-1})$ is analogously defined to $C^*(\gamma^2, R^2, \Gamma_1^2, \Gamma_2^2)$.

PROOF. Immediate from Propositions G.2 and E.1. \square

G.2 Proof of Theorem 4.2

PROOF. Immediate from Theorem G.1 by simplifying terms and using Property 4.1. \square

H PROOFS - REGRET ANALYSIS

H.1 Regret - Helper Lemmas

PROPOSITION H.1. For $n \in [N]$, and $t \in [H]$ assume,

- $\|P_{\Omega_{(T+tL,n)}^k} - P_{\Omega_{(T+HL,N)}^k}\| \leq \Delta_{(T+tL,n)}$
- $\|\hat{\beta}_{(T+tL,n)}\|_2 \leq B$, for all $\hat{\beta}_{(T+tL,n)} \in \Omega_{(T+tL,n)}^k$
- $\|\nabla c_{(T+tL,n)}(\hat{\beta}_{(T+tL,n)})\|^2 \leq D$

Then, for large enough absolute constant $C > 0$

$$\text{regret} \leq \frac{C}{2\delta} \left(B^2 + NH\delta^2 D + B^2 \sum_{n=1}^N \sum_{t=1}^H \Delta_{(T+tL,n)} \right). \quad (59)$$

PROOF. For simplicity, write $\beta^* := \beta_{(T+H \times L, N)}^*$ as in the definition of regret, let $\beta_{(T+tL,n)}^*$ be the projection of β^* onto $\Omega_{(T+tL,n)}^k$. Then for $n \in [N]$, and $t \in [H]$,

$$\begin{aligned} & (c_{(T+tL,n)}(\hat{\beta}_{(T+tL,n)}) - c_{(T+tL,n)}(\beta^*)) \\ & \leq \nabla c_{(T+tL,n)}(\hat{\beta}_{(T+tL,n)})(\hat{\beta}_{(T+tL,n)} - \beta^*), \quad \text{due to convexity of } c_{(T+tL,n)}(\cdot) \\ & = \left(\frac{\hat{\beta}_{(T+tL,n)} - \hat{\beta}_{(T+(t+1)L,n}}}{\delta} \right) (\hat{\beta}_{(T+tL,n)} - \beta^*), \quad \text{due to update definition in online-mSSA} \\ & = \frac{1}{2\delta} \left(\|\beta^* - \hat{\beta}_{(T+tL,n)}\|_2^2 - \|\beta^* - \hat{\beta}_{(T+(t+1)L,n)}\|_2^2 + \|\hat{\beta}_{(T+tL,n)} - \hat{\beta}_{(T+(t+1)L,n)}\|_2^2 \right) \\ & = \frac{1}{2\delta} \left(\|\beta^* - \hat{\beta}_{(T+tL,n)}\|_2^2 - \|\beta^* - \hat{\beta}_{(T+(t+1)L,n)}\|_2^2 + \delta^2 \|\nabla c_{(T+tL,n)}(\hat{\beta}_{(T+tL,n)})\|_2^2 \right), \end{aligned}$$

where we again use the definition of the online-mSSA. First,

$$\begin{aligned} \|\beta^* - \hat{\beta}_{(T+tL,n)}\|_2^2 &= \|\beta^* - \beta_{(T+tL,n)}^* + \beta_{(T+tL,n)}^* - \hat{\beta}_{(T+tL,n)}\|_2^2 \\ &= \|\beta^* - \beta_{(T+tL,n)}^*\|_2^2 + \|\beta_{(T+tL,n)}^* - \hat{\beta}_{(T+tL,n)}\|_2^2 + 2\langle \beta^* - \beta_{(T+tL,n)}^*, \beta_{(T+tL,n)}^* - \hat{\beta}_{(T+tL,n)} \rangle \\ &= \|\beta^* - \beta_{(T+tL,n)}^*\|_2^2 + \|\beta_{(T+tL,n)}^* - \hat{\beta}_{(T+tL,n)}\|_2^2 \end{aligned}$$

In above, $\langle \beta^* - \beta_{(T+tL,n)}^*, \beta_{(T+tL,n)}^* - \hat{\beta}_{(T+tL,n)} \rangle = 0$ due to $\beta^* - \beta_{(T+tL,n)}^*$ being orthogonal to any vector in $\Omega_{(T+tL,n)}^k$ including $\beta_{(T+tL,n)}^* - \hat{\beta}_{(T+tL,n)}^*$.

Next,

$$\begin{aligned} \|\beta^* - \hat{\beta}_{(T+(t+1)L,n)}\|_2^2 &= \|\beta^* - \beta_{(T+(t+1)L,n)}^* + \beta_{(T+(t+1)L,n)}^* - \hat{\beta}_{(T+(t+1)L,n)}\|_2^2 \\ &= \|\beta^* - \beta_{(T+(t+1)L,n)}^*\|_2^2 + \|\beta_{(T+(t+1)L,n)}^* - \hat{\beta}_{(T+(t+1)L,n)}\|_2^2 \\ &\quad + 2\langle \beta^* - \beta_{(T+(t+1)L,n)}^*, \beta_{(T+(t+1)L,n)}^* - \hat{\beta}_{(T+(t+1)L,n)} \rangle \\ &\geq \|\beta^* - \beta_{(T+(t+1)L,n)}^*\|_2^2 + \|\beta_{(T+(t+1)L,n)}^* - \hat{\beta}_{(T+(t+1)L,n)}\|_2^2 \\ &\quad + 2\langle \beta^* - \beta_{(T+(t+1)L,n)}^*, \beta_{(T+(t+1)L,n)}^* - \hat{\beta}_{(T+(t+1)L,n)} \rangle \end{aligned}$$

In above, the inequality follows since $\hat{\beta}_{(T+(t+1)L,n)}$ is projection of $\hat{\beta}_{(T+(t+1)L,n)}$ on linear sub-space $\Omega_{(T+tL,n)}^k$ which contains $\beta_{(T+(t+1)L,n)}^*$ and hence the inequality for $\|\cdot\|_2$. Hence we have,

$$\begin{aligned} 2\delta \cdot (c_{(T+tL,n)}(\hat{\beta}_{(T+tL,n)}) - c_{(T+tL,n)}(\beta^*)) \\ \leq \|\beta^* - \beta_{(T+tL,n)}^*\|_2^2 - \|\beta^* - \beta_{(T+(t+1)L,n)}^*\|_2^2 + \|\beta_{(T+tL,n)}^* - \hat{\beta}_{(T+tL,n)}\|_2^2 - \|\beta_{(T+(t+1)L,n)}^* - \hat{\beta}_{(T+(t+1)L,n)}\|_2^2 \\ - 2\langle \beta^* - \beta_{(T+(t+1)L,n)}^*, \beta_{(T+(t+1)L,n)}^* - \hat{\beta}_{(T+(t+1)L,n)} \rangle + \delta^2 \|\nabla c_{(T+tL,n)}(\hat{\beta}_{(T+tL,n)})\|_2^2 \end{aligned}$$

Summing over $n \in [N]$ and $t \in [H]$,

$$\begin{aligned} 2\delta \cdot \sum_{n=1}^N \sum_{t=1}^H (c_{(T+tL,n)}(\hat{\beta}_{(T+tL,n)}) - c_{(T+tL,n)}(\beta^*)) \\ \leq \|\beta^* - \beta_{(T+tL,n)}^*\|_2^2 + \|\beta_{(T+tL,n)}^* - \hat{\beta}_{(T+tL,n)}\|_2^2 + \sum_{n=1}^N \sum_{t=1}^H \left(\langle \beta_{(T+(t+1)L,n)}^* - \beta^*, \beta_{(T+(t+1)L,n)}^* - \hat{\beta}_{(T+(t+1)L,n)} \rangle \right. \\ \left. + \delta^2 \|\nabla c_{(T+tL,n)}(\hat{\beta}_{(T+tL,n)})\|_2^2 \right) \\ \leq 8B^2 + P\delta^2 D + \sum_{n=1}^N \sum_{t=1}^H \left(\langle \beta_{(T+(t+1)L,n)}^* - \beta^*, \beta_{(T+(t+1)L,n)}^* - \hat{\beta}_{(T+(t+1)L,n)} \rangle \right). \end{aligned}$$

For any $u \in \mathbb{R}^{L-1}$, $t \in [H]$ and using definition of $\beta_{(T+(t+1)L,n)}^*$, β^* we obtain

$$\begin{aligned} \langle \beta_{(T+(t+1)L,n)}^* - \beta^*, u \rangle &= \langle P_{\Omega_{(T+(t+1)L,n)}^k} \beta^* - P_{\Omega_{(T+HL,N)}^k} \beta^*, u \rangle \\ &\leq \|P_{\Omega_{(T+(t+1)L,n)}^k} - P_{\Omega_{(T+HL,N)}^k}\| \|\beta^*\| \|u\|. \end{aligned}$$

Hence,

$$\sum_{n=1}^N \sum_{t=1}^H \left(\langle \beta_{(T+(t+1)L,n)}^* - \beta^*, \beta_{(T+(t+1)L,n)}^* - \hat{\beta}_{(T+(t+1)L,n)} \rangle \right) \leq B^2 \sum_{n=1}^N \sum_{t=1}^H \Delta_{(T+tL,n)}.$$

□

PROPOSITION H.2 (Bounding D). Let B, D be defined as in Proposition H.1. Let $a_{(T+tL,n,j)}^i$ and $X_n(T+tL)$ be defined as in Section 4.3. Assume,

- $\max_{i \in [L-1], t \in [H+1], n \in [N], j \in [\bar{P}+t]} |a_{(T+tL,n,j)}^i| = D_1$

- $\max_{t \in [H+1], n \in [N]} |X_n(T + tL)| = D_2$

Then,

$$D \leq C \cdot k^3 \cdot B^2 \cdot D_1^4 \cdot D_2^2 \quad (60)$$

where C is an absolute constant.

PROOF.

$$\begin{aligned} \|\nabla c_{(T+tL,n)}(\hat{\beta}_{(T+tL,n)})\|_2^2 &= \|\nabla_{\hat{\beta}_{(T+tL,n)}} \left(X_n(T + tL) - \left(X_n(T + (t-1)L + 1 : T + tL - 1) \right)^T \hat{\beta}_{(T+tL,n)} \right)^2\|_2^2 \\ &= \|\nabla_{\hat{\beta}_{(T+tL,n)}} \left(X_n(T + tL) - \sum_{i=1}^k a_{(T+tL,n,j)}^i (v_{(t,n)}^i)^T \hat{\beta}_{(T+tL,n)} \right)^2\|_2^2 \\ &= \|2 \left(X_n(T + tL) - \sum_{i=1}^k a_{(T+tL,n,j)}^i (v_{(t,n)}^i)^T \hat{\beta}_{(T+tL,n)} \right) \left(\sum_{i=1}^k a_{(T+tL,n,j)}^i v_{(t,n)}^i \right)\|_2^2 \\ &\leq 4 \left((X_n(T + tL))^2 + (kBD_1)^2 \right) \left\| \left(\sum_{i=1}^k a_{(T+tL,n,j)}^i v_{(t,n)}^i \right) \right\|_2^2 \\ &\leq 4 \left((D_2)^2 + (kBD_1)^2 \right) k (D_1)^2 \end{aligned}$$

Hence,

$$D \leq C \cdot k^3 \cdot B^2 \cdot D_1^4 \cdot D_2^2$$

where C is an absolute constant. \square

H.1.1 Bounding $\Delta_{(T+tL,n)}$.

PROPOSITION H.3. Recall $\tau_{(t,n)}^1, \dots, \tau_{(t,n)}^k$ be the first k singular values of $\bar{M}_{(t,n)}^f$. Assume, for $n \in [N]$ and $t \in [H+1]$,

- $P_{\Omega_{(T+tL,n)}^k} = P_{\Omega_{(T+HL,N)}^k}$,
- Assume Properties 2.1, 2.3, 2.4 and 2.2 hold.

Let C_3 be large enough constant defined as in Theorem 4.3. Then, with probability at least $1 - 1/(NT)^4$,

$$\|P_{\Omega_{(T+tL,n)}^k} - P_{\Omega_{(T+HL,N)}^k}\| \leq C_3 \frac{\sqrt{LNH}}{\tau_{(T+tL,n)}^k - \tau_{(T+tL,n)}^{k+1} - (\sqrt{L} + \sqrt{N(P+H)})}.$$

PROOF. Let $\tilde{\tau}_{(T+tL,n)}^1, \dots, \tilde{\tau}_{(T+tL,n)}^k$ be the first k (ordered by magnitude) singular values of $\bar{Z}_{(T+tL,n)}^X$. Define $\check{Z}_{(T+tL,n)}^X \in \mathbb{R}^{L \times (N(P+H))}$, which is induced from $\bar{Z}_{(T+tL,n)}^X$, by stacking columns of all 0s to the right of it to make it of dimension $L \times (N(P+H))$. Let $E_{(T+tL,n)} := \bar{Z}_{(T,N)}^X - \check{Z}_{(T+tL,n)}^X$.

By the Davis-Kahan sin Θ theorem, we have,

$$\begin{aligned} \|P_{\Omega_{(T+tL,n)}^k} - P_{\Omega_{(T+HL,N)}^k}\| &\leq C_3 \frac{\|E_{(T+tL,n)}\|}{\tilde{\tau}_{(t,n)}^k - \tilde{\tau}_{(T+tL,n)}^{k+1}} \\ &\leq C_3 \frac{\sqrt{NLH}}{\tilde{\tau}_{(T+tL,n)}^k - \tilde{\tau}_{(T+tL,n)}^{k+1}} \end{aligned}$$

By the Cauchy Interlacing Theorem and an application of Theorem D.2 on $\bar{Z}_{(T+tL,n)}^X - \bar{M}_{(T+tL,n)}^f$, with appropriately chosen large enough $C_3 > 0$, it follows that with probability at least $1 - 1/(NT)^4$, we have that for $i \in [L-1]$

$$|\tilde{\tau}_{(T+tL,n)}^i - \tau_{(T+tL,n)}^i| \leq C_3(\sqrt{L} + \sqrt{N(P+H)}).$$

Hence,

$$C^* \frac{\sqrt{NLH}}{\tilde{\tau}_{(T+tL,n)}^k - \tilde{\tau}_{(T+tL,n)}^{k+1}} \leq C^* \frac{\sqrt{NLH}}{\tau_{(T+tL,n)}^k - \tau_{(T+tL,n)}^{k+1} - (\sqrt{L} + \sqrt{N(P+H)})}.$$

□

COROLLARY H.1. For $n \in [N]$ and $t \in [H+1]$, assume:

- Conditions of Proposition H.3 hold;
- $\tau_{(T+tL,n)}^k = \Omega\left(\sqrt{\frac{LNp}{k}}\right)$, $\tau_{(T+tL,n)}^{k+1} = 0$;
- $H = o(P)$.

Then for $n \in [N]$, $t \in [H]$, we have $\|P_{\Omega_{(T+tL,n)}^k} - P_{\Omega_{(T+HL,N)}^k}\| \leq C_3 \sqrt{\frac{kH}{P}}$.

PROOF. Using, Proposition H.3, we have

$$\|P_{\Omega_{(T+tL,n)}^k} - P_{\Omega_{(T+HL,N)}^k}\| \leq C_3 \frac{\sqrt{LNH}}{\tau_{(T+tL,n)}^k - \tau_{(T+tL,n)}^{k+1} - (\sqrt{L} + \sqrt{N(P+H)})} \leq C_3 \sqrt{\frac{kH}{P}}$$

□

H.2 Proof of Theorem 4.3

PROOF. From Propositions H.1, H.2 and Corollary H.1, we have

$$\frac{1}{NH} \text{regret} \leq C_3 k^{2.5} \left(\frac{1}{\delta} \left(\frac{1}{NH} + \sqrt{\frac{H}{P}} \right) + \delta L^2 \right), \quad (61)$$

with probability at least $1 - 1/(NT)$ by Union Bound.

Recall $L = P^{1-\epsilon_1}$, $H = P^{1-\epsilon_2}$. Then, $\frac{1}{NH} + \sqrt{\frac{H}{P}} = \frac{1}{NP^{1-\epsilon_2}} + \frac{1}{P^{0.5\epsilon_2}}$.

Setting $\delta = \frac{1}{L} \sqrt{\frac{1}{NH} + \sqrt{\frac{H}{P}}} = \frac{1}{L} \sqrt{\left(\frac{1}{NP^{1-\epsilon_2}} + \frac{1}{P^{0.5\epsilon_2}} \right)}$, we get

$$\begin{aligned} \left(\frac{1}{\delta} \left(\frac{1}{NH} + \sqrt{\frac{H}{P}} \right) + \delta L^2 \right) &= 2P^{1-\epsilon_1} \sqrt{\left(\frac{1}{NP^{1-\epsilon_2}} + \frac{1}{P^{0.5\epsilon_2}} \right)} \\ &= 2 \sqrt{\left(\frac{P^{2-2\epsilon_1}}{NP^{1-\epsilon_2}} + \frac{P^{2-2\epsilon_1}}{P^{0.5\epsilon_2}} \right)} = 2 \sqrt{\left(\frac{P^{1-2\epsilon_1+\epsilon_2}}{N} + P^{2-2\epsilon_1-0.5\epsilon_2} \right)} \end{aligned}$$

□